Table 1 Effects of intravenous angiotensin II (ANG II) on the parameters of logistic functions and regression lines of the open-loop baroreflex characteristics

	Control 1	Control 2	ANG II
Total baroreflex, CSP–AP relation			
P_1 (mmHg)	56.2 ± 7.2	56.3 ± 6.4	49.7 ± 6.2
P_2 (mmHg^{-1})	0.116 ± 0.019	0.118 ± 0.015	0.094 ± 0.013
P_3 (mmHg)	129.2 ± 3.5	124.5 ± 2.8	125.7 ± 3.2
P_4 (mmHg)	67.6 ± 4.6	69.7 ± 5.8	101.4 ± 10.9**,††
Maximum gain	1.57 ± 0.28	1.58 ± 0.22	1.20 ± 0.25
Baroreflex control of HR, CSP–HR relation			
P_1(beats/min)	41.7 ± 5.1	43.9 ± 6.2	51.2 ± 3.8
P_2 (mmHg^{-1})	0.123 ± 0.027	0.133 ± 0.018	0.099 ± 0.013
P_3 (mmHg)	131.8 ± 3.8	125.8 ± 3.6	129.1 ± 2.6
P_4 (beats/min)	391.1 ± 13.7	388.0 ± 12.6	417.4 ± 11.5**,††
Maximum slope (beats min^{-1} mmHg^{-1})	1.11 ± 0.12	1.39 ± 0.23	1.28 ± 0.19
Neural arc, CSP–SNA relation			
P_1 (%)	69.6 ± 5.7	66.5 ± 7.4	78.9 ± 9.1
P_2 (mmHg^{-1})	0.110 ± 0.016	0.124 ± 0.015	0.098 ± 0.011
P_3 (mmHg)	133.2 ± 3.8	127.3 ± 3.1	126.0 ± 3.4*
P_4 (%)	33.3 ± 5.4	35.0 ± 6.4	56.5 ± 11.5*,†
Maximum slope (%/mmHg)	1.94 ± 0.34	2.02 ± 0.33	2.04 ± 0.42
Peripheral arc, SNA–AP relation			
Slope, a (mmHg/%)	0.85 ± 0.09	0.86 ± 0.06	0.66 ± 0.10
Intercept, b (mmHg)	37.8 ± 5.2	36.9 ± 5.5	68.0 ± 10.6**,††
AP at 100% SNA (mmHg)	122.7 ± 9.9	122.7 ± 7.0	134.4 ± 4.9
Operating point			
AP (mmHg)	111.4 ± 5.0	110.3 ± 5.1	128.1 ± 4.4**,††
SNA (%)	90.6 ± 7.4	85.8 ± 2.1	94.3 ± 5.9

Data are mean and SE values

CSP Carotid sinus pressure, *AP* arterial pressure, *HR* heart rate, *SNA* sympathetic nerve activity

* $P < 0.05$ and ** $P < 0.01$ from control 1, † $P < 0.05$ and †† $P < 0.01$ from control 2

CSP, however, the baroreflex should be able to control SNA in the presence of ANG II (Fig. 3a). Lumbers et al. [29] pointed out a problem regarding the use of ANG II-induced hypertension as an input perturbation to evaluate the baroreflex.

Effects of ANG II on the baroreflex peripheral arc

The open-loop system characteristics of the baroreflex peripheral arc, assessed using the AP response as a function of SNA, approximated a straight line under both control and ANG II-treated conditions (Fig. 3b), suggesting that the splanchnic SNA may represent changes in systemic SNA that controlled the AP. ANG II significantly increased the intercept of the regression line, reflecting its direct vasoconstrictive effect (Table 1). Because the AP at 100% SNA did not differ among the three conditions, the slope could be shallower in the presence of ANG II. In other words, ANG II appears to elevate the AP to a greater extent for the lower SNA range. Although both the modulation of sympathetic neurotransmission and direct vasoconstriction contribute to the elevation of AP, the fact that ANG II enhances the sympathetic neurotransmission more with a lower stimulation frequency [30, 31] may, in part, account for the greater ANG II-induced increase in AP for the lower SNA range.

Effects of ANG II on the open-loop sympathetic baroreflex control of HR

The baroreflex control of HR showed changes similar to those observed for SNA. Intravenous ANG II increased both the minimum and maximum HR while not significantly affecting the response range of HR or the maximum slope of the response (Fig. 2b; Table 1). The midpoint in CSP was not changed by ANG II. Therefore, the open-loop baroreflex control of HR shifted upward to higher HR values without a concomitant rightward shift to higher CSP values in the present study. In contrast, previous studies reported a rightward shift in the baroreflex control of HR toward higher input pressure values during acute [11, 32] and chronic [33] administration of ANG II in conscious rabbits. Reid and Chou [32] indicated that the inhibition of vagal tone to the heart played a significant role in resetting the baroreflex control of HR in conscious rabbits. It is likely that the rightward shift in the baroreflex control of

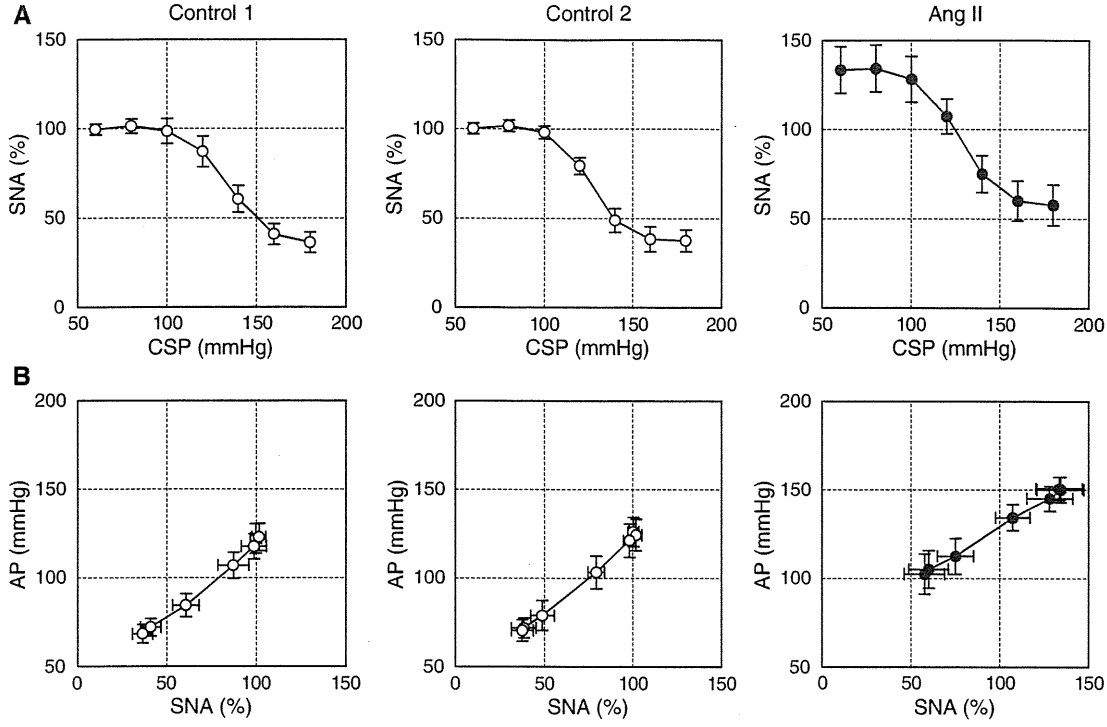

Fig. 3 **a** Averaged input–output relation of the baroreflex neural arc or the arterial baroreflex control of SNA. SNA decreased in response to an increase in the CSP. ANG II increased SNA, while the range of the SNA response was preserved. **b** Averaged input–output relation of the baroreflex peripheral arc. AP increased in response to an increase in SNA. ANG II increased the AP, an effect that was greater for lower SNA

HR by ANG II was not observed in the present study because the vagal nerves were sectioned.

Limitations

First, we performed the experiments in anesthetized animals, and comparisons with results obtained in conscious animals should be made carefully. Circulating levels of ANG II may vary under anesthesia, which could have affected the present results. For instance, reported plasma ANG II concentration in pithed rats is approximately 400 pg/ml [16], which exceeds the plasma ANG II concentration reported in rats with heart failure [34]. Second, although the dose of ANG II used in the present study was within or below those used in previous studies in rats [12, 16, 17], Brown et al. demonstrated that intravenous ANG II at 20 and 270 ng kg^{-1} min^{-1} increased the plasma ANG II concentration from approximately 80 pg/ml to 140 and 2,000 pg/ml, respectively [35]. Based on those data, the plasma ANG II concentration might have been increased beyond a physiologically relevant range to approximately 1,200 pg/ml in the present study. Therefore, the observed effect of ANG II on the arterial baroreflex should be interpreted as pharmacologic. Effects of circulating ANG II can be different when examined in different doses. Third, there was large variation in HR values among the animals (Fig. 2b). Increasing the number of animals would reduce this variation. Nevertheless, data from the eight rats was sufficient to perform statistical analyses and draw reasonable conclusions. Fourth, we occluded the common carotid arteries to isolate the carotid sinuses. Although the vertebral arteries were kept intact and the effects of ANG II were examined using the same preparation, the possibility cannot be ruled out that the carotid occlusion affected the present results. Finally, we cut the vagal nerves to obtain the open-loop condition for the carotid sinus baroreflex. Further studies are needed to clarify the effects of ANG II on the baroreflex control of the cardiovascular system through the vagal system.

Conclusion

The present study indicates that high circulating levels of ANG II significantly increased splanchnic SNA but did not acutely attenuate the range of arterial baroreflex control of SNA. The ranges of the total baroreflex response and the baroreflex control of HR were also preserved during ANG

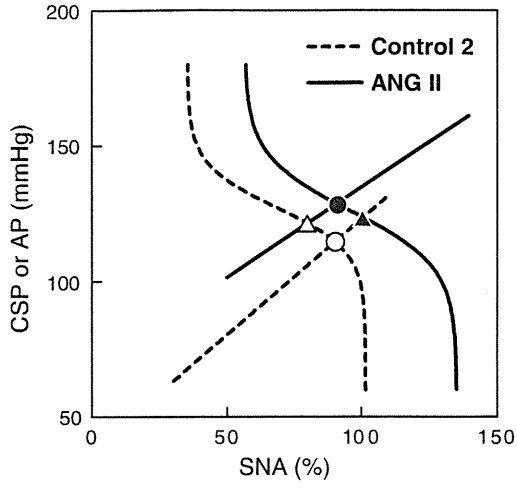

Fig. 4 Equilibrium diagrams between the arterial baroreflex neural and peripheral arcs. The *dashed* and *solid curves* represent the open-loop characteristics of the baroreflex neural arc under the control and ANG II-treated conditions, respectively. The *dashed* and *solid lines* represent the open-loop characteristics of the baroreflex peripheral arc under the control and ANG II-treated conditions, respectively. The *open circle* indicates the closed-loop operating point under the control condition. ANG II causes an upward shift in the peripheral arc. If ANG II does not affect the neural arc, the closed-loop operating point would be at the point depicted by the *open triangle*. In this case, the estimation of baroreflex control of SNA based on the closed-loop operating points (the *open circle* and *open triangle*) approximates the slope of the baroreflex neural arc (*dashed curve*). ANG II, however, causes a rightward shift in the neural arc. Thus, the estimation of the baroreflex control of SNA based on closed-loop operating points (the *open* and *filled circles*) does not match the slope of the neural arc under either the control (*dashed curve*) or ANG II-treated condition (*solid curve*)

II administration. ANG II does modify the arterial baroreflex in that it increases SNA at a given baroreceptor pressure level but does not appear to attenuate the range of arterial baroreflex control of SNA, HR or AP.

Acknowledgments This study was supported by Health and Labour Sciences Research Grants (H18-nano-Ippan-003, H19-nano-Ippan-009, H20-katsudo-Shitei-007, and H21-nano-Ippan-005) from the Ministry of Health, Labour and Welfare of Japan; by a Grant-in-Aid for Scientific Research (No. 20390462) from the Ministry of Education, Culture, Sports, Science and Technology of Japan; and by the Industrial Technology Research Grant Program from the New Energy and Industrial Technology Development Organization (NEDO) of Japan.

References

1. Ikeda Y, Kawada T, Sugimachi M, Kawaguchi O, Shishido T, Sato T, Miyano H, Matsuura W, Alexander J Jr, Sunagawa K (1996) Neural arc of baroreflex optimizes dynamic pressure regulation in achieving both stability and quickness. Am J Physiol 271:H882–H890
2. Kawada T, Yamamoto K, Kamiya A, Ariumi H, Michikami D, Shishido T, Sunagawa K, Sugimachi M (2005) Dynamic characteristics of carotid sinus pressure-nerve activity transduction in rabbits. Jpn J Physiol 55:157–163
3. Sato T, Kawada T, Shishido T, Miyano H, Inagaki M, Miyashita H, Sugimachi M, Kneupfer MM, Sunagawa K (1998) Dynamic transduction properties of in situ baroreceptors of rabbit aortic depressor nerve. Am J Physiol Heart Circ Physiol 274:H358–H365
4. Chapleau MW, Abboud FM (1987) Contrasting effects of static and pulsatile pressure on carotid baroreceptor activity in dogs. Circ Res 61:648–658
5. Kawada T, Fujiki N, Hosomi H (1992) Systems analysis of the carotid sinus baroreflex system using a sum-of-sinusoidal input. Jpn J Physiol 42:15–34
6. Kawada T, Yanagiya Y, Uemura K, Miyamoto T, Zheng C, Li M, Sugimachi M, Sunagawa K (2002) Input-size dependence of the baroreflex neural arc transfer characteristics. Am J Physiol Heart Circ Physiol 284:H404–H415
7. Kawada T, Zheng C, Yanagiya Y, Uemura K, Miyamoto T, Inagaki M, Shishido T, Sugimachi M, Sunagawa K (2002) High-cut characteristics of the baroreflex neural arc preserve baroreflex gain against pulsatile pressure. Am J Physiol Heart Circ Physiol 282:H1149–H1156
8. Reid IA (1992) Interactions between ANG II, sympathetic nervous system, and baroreceptor reflexes in regulation of blood pressure. Am J Physiol Endocrinol Metab 262:E763–E778
9. Sanderford MG, Bishop VS (2000) Angiotensin II acutely attenuates range of arterial baroreflex control of renal sympathetic nerve activity. Am J Physiol Heart Circ Physiol 279:H1804–H1812
10. McMullan S, Goodchild AK, Pilowsky PM (2007) Circulating angiotensin II attenuates the sympathetic baroreflex by reducing the barosensitivity of medullary cardiovascular neurons in the rat. J Physiol 582:711–722
11. Kumagai K, Reid IA (1994) Angiotensin II exerts differential actions on renal nerve activity and heart rate. Hypertension 24:451–456
12. Tan PS, Killinger S, Horiuchi J, Dampney RA (2007) Baroreceptor reflex modulation by circulating angiotensin II is mediated by AT_1 receptors in the nucleus tractus solitarius. Am J Physiol Regul Integr Comp Physiol 293:R2267–R2278
13. Zucker IH (2006) Novel mechanisms of sympathetic regulation in chronic heart failure. Hypertension 48:1005–1011
14. Shoukas AA, Callahan CA, Lash JM, Haase EB (1991) New technique to completely isolate carotid sinus baroreceptor regions in rats. Am J Physiol Heart Circ Physiol 260:H300–H303
15. Sato T, Kawada T, Miyano H, Shishido T, Inagaki M, Yoshimura R, Tatewaki T, Sugimachi M, Alexander J Jr, Sunagawa K (1999) New simple methods for isolating baroreceptor regions of carotid sinus and aortic depressor nerves in rats. Am J Physiol Heart Circ Physiol 276:H326–H332
16. Grant TL, McGrath JC (1988) Interactions between angiotensin II, sympathetic nerve-mediated pressor response and cyclo-oxygenase products in the pithed rat. Br J Pharmacol 95:1220–1228
17. Haywood JR, Fink GD, Buggy J, Phillips MI, Brody MJ (1980) The area postrema plays no role in the pressor action of angiotensin in the rat. Am J Physiol Heart Circ Physiol 239:H108–H113
18. Kent BB, Drane JW, Blumenstein B, Manning JW (1972) A mathematical model to assess changes in the baroreceptor reflex. Cardiology 57:295–310
19. Glantz SA (2002) Primer of biostatistics, 5th edn. McGraw-Hill, New York
20. Mohrman DE, Heller LJ (2006) Cardiovascular physiology, 6th edn. McGraw Hill, New York, pp 172–177
21. Sato T, Kawada T, Inagaki M, Shishido T, Takaki H, Sugimachi M, Sunagawa K (1999) New analytic framework for

understanding sympathetic baroreflex control of arterial pressure. Am J Physiol Heart Circ Physiol 276:H2251–H2261
22. Kawada T, Shishido T, Inagaki M, Zheng C, Yanagiya Y, Uemura K, Sugimachi M, Sunagawa K (2002) Estimation of baroreflex gain using a baroreflex equilibrium diagram. Jpn J Physiol 52:21–29
23. Kashihara K, Takahashi Y, Chatani K, Kawada T, Zheng C, Li M, Sugimachi M, Sunagawa K (2003) Intravenous angiotensin II does not affect dynamic baroreflex characteristics of the neural or peripheral arc. Jpn J Physiol 53:135–143
24. Sanderford MG, Bishop VS (2002) Central mechanisms of acute ANG II modulation of arterial baroreflex control of renal sympathetic nerve activity. Am J Physiol Heart Circ Physiol 282:H1592–H1602
25. Fukiyama K (1972) Central action of angiotensin and hypertension—increased central vasomotor outflow by angiotensin. Jpn Circ J 36:599–602
26. Guo GB, Abboud FM (1984) Angiotensin II attenuates baroreflex control of heart rate and sympathetic activity. Am J Physiol Heart Circ Physiol 246:H80–H89
27. Kamiya A, Kawada T, Yamamoto K, Michikami D, Ariumi H, Uemura K, Zheng C, Shimizu S, Aiba T, Miyamoto T, Sugimachi M, Sunagawa K (2005) Resetting of the arterial baroreflex increases orthostatic sympathetic activation and prevents postural hypotension in rabbits. J Physiol 566:237–246
28. Yamamoto K, Kawada T, Kamiya A, Takaki H, Miyamoto T, Sugimachi M, Sunagawa K (2004) Muscle mechanoreflex induces the pressor response by resetting the arterial baroreflex neural arc. Am J Physiol Heart Circ Physiol 286:H1382–H1388
29. Lumbers ER, McCloskey DI, Potter EK (1979) Inhibition by angiotensin II of baroreceptor-evoked activity in cardiac vagal efferent nerves in the dog. J Physiol 294:69–80
30. Hughes J, Roth RH (1971) Evidence that angiotensin enhances transmitter release during sympathetic nerve stimulation. Br J Phrmacol 41:239–255
31. Zimmerman BG, Gomer SK, Liao JC (1972) Action of angiotensin on vascular adrenergic nerve endings: facilitation of norepinephrine release. Federation Proc 31:1344–1350
32. Reid IA, Chou L (1990) Analysis of the action of angiotensin II on the baroreflex control of heart rate in conscious rabbits. Endocrinology 126:2749–2756
33. Brooks VL (1995) Chronic infusion of angiotensin II resets baroreflex control of heart rate by an arterial pressure-independent mechanism. Hypertension 26:420–424
34. Schunkert H, Tang SS, Litwin SE, Diamant D, Riegger G, Dzau VJ, Ingelfinger JR (1993) Regulation of intrarenal and circulating renin–angiotensin systems in severe heart failure in the rat. Cardiovasc Res 27:731–735
35. Brown AJ, Casals-Stenzel J, Gofford S, Lever AF, Morton JJ (1981) Comparison of fast and slow pressor effects of angiotensin II in the conscious rat. Am J Physiol Heart Circ Physiol 241:H381–H388

Life Sciences 85 (2009) 597–601

Contents lists available at ScienceDirect

Life Sciences

journal homepage: www.elsevier.com/locate/lifescie

Detection of endogenous acetylcholine release during brief ischemia in the rabbit ventricle: A possible trigger for ischemic preconditioning

Toru Kawada [a,*], Tsuyoshi Akiyama [b], Shuji Shimizu [a], Atsunori Kamiya [a], Kazunori Uemura [a], Meihua Li [a], Mikiyasu Shirai [b], Masaru Sugimachi [a]

[a] Department of Cardiovascular Dynamics, Advanced Medical Engineering Center, National Cardiovascular Center Research Institute, Japan
[b] Department of Cardiac Physiology, National Cardiovascular Center Research Institute, Japan

ARTICLE INFO

Article history:
Received 1 July 2009
Accepted 25 August 2009

Keywords:
Acetylcholine
Cardiac microdialysis
Vagal stimulation
Coronary artery occlusion
Rabbits

ABSTRACT

Aims: To examine endogenous acetylcholine (ACh) release in the rabbit left ventricle during acute ischemia, ischemic preconditioning and electrical vagal stimulation.
Main methods: We measured myocardial interstitial ACh levels in the rabbit left ventricle using a cardiac microdialysis technique. In Protocol 1 ($n=6$), the left circumflex coronary artery (LCX) was occluded for 30 min and reperfused for 30 min. In Protocol 2 ($n=5$), the LCX was temporarily occluded for 5 min. Ten minutes later, the LCX was occluded for 30 min and reperfused for 30 min. In Protocol 3 ($n=5$), bilateral efferent vagal nerves were stimulated at 20 Hz and 40 Hz (10 V, 1-ms pulse duration).
Key findings: In Protocol 1, a 30-min coronary occlusion increased the ACh level from 0.39 ± 0.15 to 7.0 ± 2.2 nM (mean ± SE, $P<0.01$). In Protocol 2, a 5-min coronary occlusion increased the ACh level from 0.33 ± 0.07 to 0.75 ± 0.11 nM ($P<0.05$). The ACh level returned to 0.48 ± 0.10 nM during the interval. After that, a 30-min coronary occlusion increased the ACh level to 2.4 ± 0.49 nM ($P<0.01$). In Protocol 3, vagal stimulation at 20 Hz and 40 Hz increased the ACh level from 0.29 ± 0.06 to 1.23 ± 0.48 ($P<0.05$) and 2.44 ± 1.13 nM ($P<0.01$), respectively.
Significance: Acute ischemia significantly increased the ACh levels in the rabbit left ventricle, which appeared to exceed the vagal stimulation-induced ACh release. Brief ischemia as short as 5 min can also increase the ACh level, suggesting that endogenous ACh release can be a trigger for ischemic preconditioning.

Introduction

Although ventricular vagal innervation is sparser than that observed in the atrium, we have previously demonstrated that electrical vagal stimulation and acute myocardial ischemia significantly increased myocardial interstitial acetylcholine (ACh) levels in the feline left ventricle (Kawada et al. 2000, 2001, 2006a,b, 2007). Potential differences between species, however, suggest that data obtained from the feline left ventricle may not be directly extrapolated to ventricular vagal innervation in other species (Brown 1976; Kilbinger and Löffelholz 1976). Compared with the feline heart, the rabbit heart is more frequently analyzed in investigations of myocardial ischemia and ischemic preconditioning. For instance, Qin et al. (2003) used isolated rabbit hearts to demonstrate that ACh and adenosine induce ischemic preconditioning mimetic effects through different signaling pathways. In our previous study, vagal stimulation increased the level of tissue inhibitor of metalloproteinase-1 (TIMP-1) and reduced the level of endogenous active matrix metalloproteinase-9 (MMP-9) during ischemia–reperfusion injury in the rabbit left ventricle (Uemura et al. 2007). Despite its potential cardioprotective effects against myocardial ischemia, the profile of endogenous ACh release in the rabbit left ventricle is poorly understood *in vivo* owing to the difficulty in detecting low levels of myocardial interstitial ACh. Quantification of endogenous ACh release during myocardial ischemia and electrical vagal stimulation would help understand the potential cardioprotective effects of vagal stimulation. In the present study, we examined the effects of acute myocardial ischemia, ischemic preconditioning, and electrical vagal stimulation on myocardial interstitial ACh levels in the rabbit left ventricle *in vivo* using an improved high-performance liquid chromatography (HPLC) system that allowed us to detect low concentrations of ACh (Shimizu et al. 2009).

Materials and methods

Surgical preparation and protocols

Animal care was conducted in accordance with the *Guiding Principles for the Care and Use of Animals in the Field of Physiological Sciences*, which has been approved by the Physiological Society of

* Corresponding author. Department of Cardiovascular Dynamics, Advanced Medical Engineering Center, National Cardiovascular Center Research Institute, 5-7-1 Fujishirodai, Suita, Osaka 565-8565, Japan. Tel.: +81 6 6833 5012x2427; fax: +81 6 6835 5403.
E-mail address: torukawa@res.ncvc.go.jp (T. Kawada).

0024-3205/$ – see front matter © 2009 Published by Elsevier Inc.
doi:10.1016/j.lfs.2009.08.015

Japan. Japanese white rabbits weighing 2.5 kg to 3.1 kg (2.8 ± 0.1 kg, mean ± SE) were anesthetized via intravenous administration of pentobarbital sodium (30–35 mg/kg) through a marginal ear vein. The animals were ventilated mechanically with room air mixed with oxygen. The anesthetic condition was maintained using a continuous intravenous infusion of urethane (125 mg kg^{-1} h^{-1}) and α-chloralose (20 mg kg^{-1} h^{-1}) through a catheter inserted in the right femoral vein. Mean arterial pressure (AP) was measured using a catheter inserted in the right femoral artery. Heart rate (HR) was measured from an electrocardiogram obtained using a cardiotachometer. The animal was placed in a lateral position, and the left fourth and fifth ribs were partially resected to allow access to the heart. The heart was suspended in a pericardial cradle.

In Protocol 1 ($n = 6$), which was designed to examine the effects of acute myocardial ischemia and reperfusion, a 3-0 silk suture was passed around a branch of the left circumflex coronary artery (LCX); both ends were passed through a polyethylene tube to make a snare to occlude the artery. A dialysis probe was implanted into the anterolateral free wall of the left ventricle perfused by the LCX. After collecting a baseline dialysate sample, the LCX was occluded for 30 min and reperfused for 30 min. After the ischemia–reperfusion protocol was finished, the LCX was occluded again and a 5-ml bolus of 1% methylene blue was injected intravenously to confirm that the dialysis probe had been implanted within the area at risk for myocardial ischemia.

In Protocol 2 ($n = 5$), which was designed to examine the effects of ischemic preconditioning (*i.e.*, a brief ischemic event preceding a major ischemic event), a 3-0 silk suture was passed around a branch of the LCX and both ends were passed through a polyethylene tube to make a snare. Two dialysis probes were implanted into the anterolateral free wall of the left ventricle perfused by the LCX; the probes were separated by at least 5 mm. Combining the dialysate samples obtained from the two dialysis probes increased the time resolution of the ACh measurement. After collecting a baseline dialysate sample, the LCX was temporarily occluded for 5 min which was followed by a 10-min interval. The LCX was then occluded for 30 min and reperfused for 30 min. After the ischemia–reperfusion protocol was completed, the LCX was occluded again and a 5-ml bolus of 1% methylene blue was injected intravenously to confirm that the two dialysis probes had been implanted within the area at risk for myocardial ischemia.

In Protocol 3 ($n = 5$), which was designed to examine the effects of electrical vagal stimulation, the vagus nerves were exposed and sectioned at the neck. Each sectioned vagus nerve was placed on a pair of bipolar platinum electrodes to stimulate the efferent vagus nerve. The nerve and the electrodes were fixed using silicone glue (Kwik-Sil, World Precision Instruments, Sarasota, FL, USA). Two dialysis probes were implanted into the anterolateral free wall of the left ventricle; the probes were separated by at least 5 mm. Dialysate samples obtained from the two dialysis probes were analyzed separately. After collecting baseline dialysate samples, the vagus nerves were stimulated at 20 Hz for 15 min and 40 Hz for 15 min. The stimulation amplitude was 10 V and the pulse duration was 1 ms. The 40-Hz stimulation often caused an initial cardiac arrest for a few seconds and was considered to be the most intensive stimulation in the present experimental settings. The 20-Hz stimulation was arbitrarily selected at a half of the maximum stimulation rate to observe the dependence of the ACh release on the stimulation rate.

At the end of each protocol, the experimental animals were sacrificed with an overdose of intravenous pentobarbital sodium. We performed a postmortem examination and confirmed that the dialysis probe(s) had been implanted within the left ventricular myocardium.

Dialysis technique

We measured dialysate concentrations of ACh as indices of myocardial interstitial ACh levels. The materials and properties of the dialysis probe have been described previously (Akiyama et al. 1994). Briefly, we designed a transverse dialysis probe. A dialysis fiber (length, 8 mm; outer diameter, 310 μm; inner diameter, 200 μm; PAN-1200, 50,000-Da molecular-weight cutoff, Asahi Chemical, Japan) was glued at both ends to polyethylene tubes (length, 25 cm; outer diameter, 500 μm; inner diameter, 200 μm). The dialysis probe was perfused at a rate of 2 μl/min with Ringer's solution containing a cholinesterase inhibitor eserine (100 μM). Dialysate sampling was started from 2 h after probe implantation. In Protocols 1 and 3, one sampling period was set at 15 min, which yielded a sample volume of 30 μl. The actual dialysate sampling lagged behind a given collection period by 5 min owing to the dead space volume between the dialysis membrane and collecting tube. In Protocol 2, one sampling period was set at 5 min to increase the time resolution during the ischemic preconditioning, and dialysate samples from the two dialysis probes were combined to yield a sample volume of 20 μl. The sampling period was changed to 10 min during the main ischemic event to reduce the total number of samples. The amount of ACh in the dialysate was measured using an HPLC system with electrochemical detection (Eicom, Japan) adjusted to measure low levels of ACh (Shimizu et al. 2009). The concentration of ACh was calculated taking the sample volume in account.

Statistical analysis

All data are presented as the mean and SE values. We performed repeated-measures analysis of variance, followed by a Tukey test for all pairwise, multiple comparisons to examine changes in the ACh levels (Glantz 2002). Because the variance of measured ACh levels increased with their mean, statistical analysis was performed after logarithmic conversion of the ACh data (Snedecor and Cochran 1989). The AP and HR data were examined using repeated-measures analysis of variance, followed by a Dunnett's test for multiple comparisons against a single control (Glantz 2002). In Protocols 1 and 3, the baseline value was treated as the single control. In Protocol 2, the value measured just before the main ischemic event was treated as the single control. In all of the statistical analyses, differences were considered significant when $P < 0.05$.

Results

In Protocol 1, the myocardial interstitial ACh levels significantly increased during ischemia compared with the baseline value (Fig. 1). Although the ACh levels declined during reperfusion, they were still significantly higher than the baseline value. Changes in AP and HR are summarized in Table 1. Although AP did not change significantly during ischemia, it decreased significantly throughout the reperfusion period. The HR increased significantly after 30 min of ischemia, and remained high during the reperfusion period with the exception of the last data point.

In Protocol 2, the LCX was occluded for 5 min (ischemic preconditioning) and released for 10 min before the major ischemic event. The brief 5-min occlusion significantly increased the myocardial interstitial ACh level compared with the baseline value (Fig. 2). The ACh levels during the interval between the brief occlusion and the major occlusion did not differ from the baseline value. The ACh levels increased significantly during the major ischemic event compared with the baseline value. Although the ACh levels declined during reperfusion, they were still significantly higher than the baseline value. Changes in AP and HR are summarized in Table 2. Neither AP nor HR changed significantly compared with the respective control values measured after the 10-min middle interval.

In Protocol 3, electrical vagal stimulation significantly increased the myocardial interstitial ACh levels (Fig. 3). The ACh levels returned close to the baseline value just after vagal stimulation was terminated. The AP and HR values were significantly reduced by vagal stimulation (Table 3).

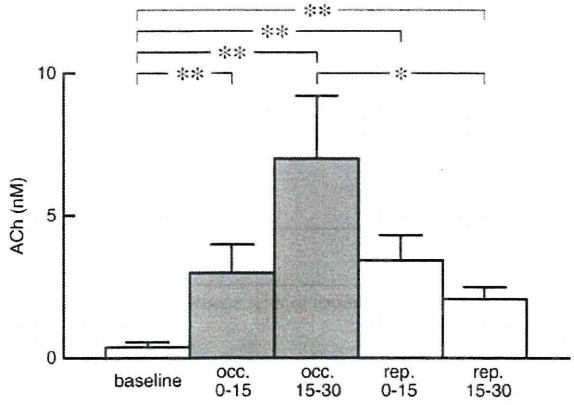

Fig. 1. Changes in the myocardial interstitial ACh levels in Protocol 1. The left circumflex coronary artery was occluded for 30 min and reperfused for 30 min. occ: occlusion; rep: reperfusion. Data are shown as the mean + SE ($n=6$). $^{*}P<0.05$ and $^{**}P<0.01$; Tukey test.

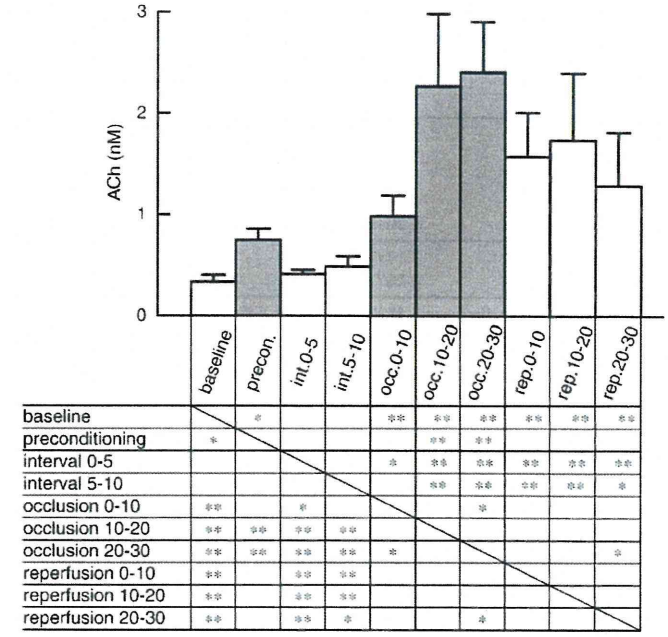

Fig. 2. Changes in the myocardial interstitial ACh levels in Protocol 2. The left circumflex coronary artery was occluded for 5 min. Ten minutes later, the left circumflex coronary artery was occluded for 30 min and reperfused for 30 min. precon: preconditioning; int: interval; occ: occlusion; rep: reperfusion. Data are shown as the mean + SE ($n=5$). $^{*}P<0.05$ and $^{**}P<0.01$; Tukey test.

Discussion

Effects of acute ischemia on myocardial interstitial ACh levels

Acute myocardial ischemia significantly increased myocardial interstitial ACh levels in the ischemic region (Fig. 1). To our knowledge, this is the first report demonstrating ischemia-induced ACh release in the rabbit left ventricle *in vivo*. Because electrical vagal stimulation increased the myocardial interstitial ACh levels (Fig. 3), centrally mediated activation of the efferent vagus nerve could contribute to these effects. LCX occlusion, however, did not decrease the HR significantly (Table 1), suggesting that centrally mediated vagal activation did not have a marked role in the present study. In a previous study, acute myocardial ischemia increased myocardial interstitial ACh levels in vagotomized cats, suggesting an important role of a local release mechanism that is independent of efferent vagal activity (Kawada et al. 2000). Intracellular Ca^{2+} mobilization related to cation-selective stretch-activated channels is thought to be involved in this local release mechanism (Kawada et al. 2000, 2006b). A similar local mechanism may be responsible for ischemia-induced ACh release in the rabbit left ventricle.

In our previous study, topical perfusion of ACh through a dialysis probe increased TIMP-1 levels in the rabbit left ventricle (Uemura et al. 2007). The production of TIMP-1 reduces endogenous levels of active MMP-9, which can limit ventricular remodeling following myocardial ischemia and reperfusion. Whether ischemia-induced ACh release can induce such an anti-remodeling effect remains unanswered, however, because reperfusion reduced the myocardial interstitial ACh levels toward the baseline value. Whether prolonged ischemia for more than 30 min induces sustained elevations of ACh levels is an interesting topic for future studies.

The ACh levels were decreased toward the baseline value upon reperfusion, probably by the washout of ACh from the interstitial fluid. In the case of myocardial interstitial myoglobin levels, the reperfusion further increases the myoglobin levels, suggesting an occurrence of reperfusion injury to the myocardium (Kitagawa et al. 2005). Reoxygenation upon reperfusion rapidly restores the ATP synthesis, which can cause hypercontracture of myofibrils and undesired cytoskeletal lesions (Piper et al. 2004). Because the vagal nerve endings do not have contractile elements, the hypercontracture-induced cell injury does not occur, and the further release of ACh may have been prevented.

Effects of ischemic preconditioning on myocardial interstitial ACh levels

Ischemic preconditioning is a phenomenon in which a brief ischemic event makes the heart resistant to a subsequent ischemic insult (Murry et al. 1986). Acetylcholine, bradykinin, and adenosine are endogenous substances that can induce ischemic preconditioning mimetic effects in the rabbit heart (Liu et al. 1991; Qin et al. 2003; Krieg et al. 2004). In a previous study, we showed that a 5-min ischemic event increased myocardial interstitial ACh levels in the feline ventricle (Kawada et al. 2002). Ischemic preconditioning, however, is not frequently examined in the feline ventricle, making interpretation of these results difficult. In the present study, a 5-min ischemic event caused a significant increase in the ACh level in the rabbit left ventricle (Fig. 2), suggesting that brief ischemia-induced ACh release may serve as a trigger for the ischemic preconditioning. Krieg et al. (2004) demonstrated that ACh triggers preconditioning by sequentially activating Akt and nitric oxide synthase to produce reactive oxygen species. An acetylcholine-induced preconditioning mimetic effect has also been observed in canine (Yao and Gross 1993; Przyklenk and Kloner 1995) and rat (Richard et al. 1995) models.

Table 1
Mean arterial pressure (AP) and heart rate (HR) obtained during Protocol 1 ($n=6$).

	Baseline	Occlusion 5 min	Occlusion 15 min	Occlusion 30 min	Reperfusion 5 min	Reperfusion 15 min	Reperfusion 30 min
AP(mm Hg)	82 ± 4	77 ± 4	72 ± 5	75 ± 5	72 ± 5*	70 ± 4*	70 ± 2**
HR (beats/min)	247 ± 16	264 ± 14	265 ± 13	280 ± 10**	278 ± 9*	277 ± 8*	274 ± 9

Data are shown as the mean ± SE. $^{*}P<0.05$ and $^{**}P<0.01$ vs. baseline using Dunnett's test.

Table 2
Mean arterial pressure (AP) and heart rate (HR) obtained during Protocol 2 ($n=5$).

	Baseline	Preconditioning 5 min	Interval 5 min	Interval 10 min	Occlusion 5 min	Occlusion 10 min
AP(mm Hg)	83±5	77±5	78±4	80±4	78±5	78±5
HR(beats/min)	277±7	282±8	282±7	284±5	285±5	286±6
	Occlusion 20 min	Occlusion 30 min	Reperfusion 5 min	Reperfusion 10 min	Reperfusion 20 min	Reperfusion 30 min
AP(mm Hg)	77±4	78±5	77±5	78±5	77±3	79±3
HR(beats/min)	287±5	289±6	290±5	289±5	290±6	293±5

Data are shown as the mean±SE. No significant differences relative to control values (the value 10 min after the preconditioning) were observed based on Dunnett's test.

In a previous study examining the feline ventricle (Kawada et al. 2002), brief ischemia significantly decreased the HR, highlighting the presence of a significant vagal reflex from the heart. Vagotomy abolished the ACh release induced by brief ischemia in that study, suggesting an important role of centrally mediated vagal activation. The vagal reflex from the heart, however, shows regional differences and varies among species (Thames et al. 1978; Kawada et al. 2007). In the present study, brief ischemia did not decrease the HR significantly (Table 2), suggesting that centrally mediated vagal activation was not a major factor for the brief ischemia-induced ACh release in the rabbit heart.

Rabbits exhibit marked effects from ischemic preconditioning, including reduced infarct size (Cohen et al. 1991; Cason et al. 1997). Although whether the ACh release induced by the brief ischemic event exerted cardioprotective effects was not examined in the present study, there was a notable difference in the changes in AP observed with Protocol 1 and Protocol 2. Although AP decreased significantly upon reperfusion in Protocol 1 (Table 1), it did not change significantly during the major ischemic event in Protocol 2 (Table 2), possibly reflecting preserved cardiac function as a result of the ischemic preconditioning.

Effects of electrical vagal stimulation on myocardial interstitial ACh levels

In the feline left ventricle, electrical vagal stimulation at 20 Hz (10 V, 1-ms pulse duration) increases myocardial interstitial ACh levels to approximately 20 nM as measured with a dialysis fiber 13 mm in length (Kawada et al. 2000). In contrast, electrical vagal stimulation at 20 Hz in the rabbit left ventricle (10 V, 1-ms pulse duration) increased the ACh levels to approximately 1.2 nM as measured with a dialysis fiber 8 mm long (Fig. 3). The small increase in the ACh level detected during electrical vagal stimulation may indicate that vagal innervation is much sparser in the rabbit ventricle

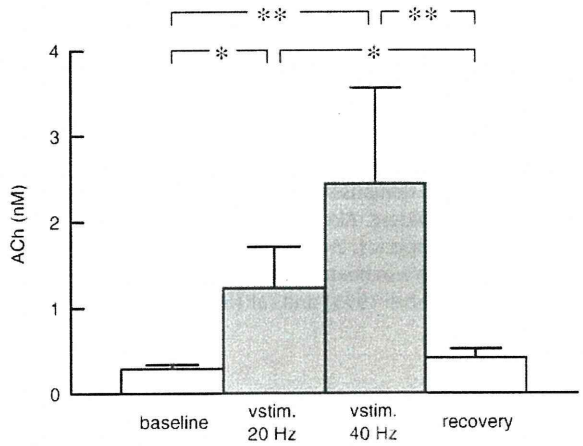

Fig. 3. Changes in the myocardial interstitial ACh levels in Protocol 3. The bilateral efferent vagus nerves were stimulated at 20 Hz for 15 min and 40 Hz for 15 min. Data are shown as the mean + SE ($n=10$, 2 samples from each of the 5 animals). *$P<0.05$ and **$P<0.01$; Tukey test.

than in the feline ventricle. In a previous study that used a dialysis fiber 4 mm in length, right vagal stimulation at 20 Hz increased the dialysate ACh concentration from 0.4±0.2 nM to 0.9±0.3 nM, whereas left vagal stimulation at 20 Hz increased it from 0.3±0.1 nM to 1.0±0.4 nM in the rabbit right ventricle (Shimizu et al. 2009). Considering the bilateral stimulation and fiber length of 8 mm in the present study, the vagal innervation of the left ventricle may be comparable to or slightly sparser than that of the right ventricle.

The dialysis fiber differed in length among studies due to anatomical restrictions related to the fiber implantation procedure (*i.e.*, size of the heart etc.). If we consider diffusive processes alone, the relative recovery (RR) can be expressed as:

$$RR = \frac{C_{inside}}{C_{outside}} = 1-\exp\left(-k\frac{A}{F}\right) = 1-\exp\left(-k\frac{mL}{F}\right)$$

where C_{inside} and $C_{outside}$ are the ACh concentrations inside and outside the dialysis fiber; A is the surface area of the dialysis membrane, which can be proportional to the fiber length L with a coefficient m; F is a perfusion flow rate; and k is the mass transfer coefficient (Ståhle 1991). The *in vitro* RR for ACh is approximately 70% with $F=2$ µl/min and $L=13$ mm (Akiyama et al. 1994), which yields $km=0.1852$. Using this value, the *in vitro* RR would be approximately 52% for $L=8$ mm and 31% for $L=4$ mm. Although these values provide some clues to speculate the effects of fiber length on the detected ACh concentrations, they cannot be directly extrapolated to the present results, because k should be different in *in vivo* conditions.

The physiological significance of vagal innervation of the left ventricle is controversial, because fixed-rate atrial pacing abolishes vagally induced inhibition of left ventricular contractility in an experimental setting without significant background sympathetic tone (Matsuura et al. 1997). On the other hand, when the cardiac sympathetic nerve is activated, vagal stimulation can reduce ventricular contractility even under fixed-rate atrial pacing by antagonizing the sympathetic effect (Nakayama et al. 2001). In addition, vagal stimulation suppresses myocardial interstitial myoglobin release during acute myocardial ischemia in anesthetized cats (Kawada et al. 2008). Chronic vagal stimulation improves the survival rate of rat models of chronic heart failure after myocardial infarction (Li et al. 2004). These lines of evidence suggest that vagal innervation of the left ventricle may be of therapeutic significance.

An unresolved question regarding the cardioprotective effects of vagal stimulation is that a large quantity of ACh is released in the ischemic region without vagal stimulation (Fig. 1). In the present

Table 3
Mean arterial pressure (AP) and heart rate (HR) obtained during Protocol 3 ($n=5$).

	Baseline	Vagal stimulation 20 Hz	Vagal stimulation 40 Hz	Recovery
AP (mm Hg)	100±3	59±9**	54±9**	86±5
HR (beats/min)	322±14	126±5**	100±8**	311±8

Data are shown as the mean±SE. **$P<0.01$ vs. baseline based on Dunnett's test.

study, vagal stimulation at 20-Hz lowered the HR by approximately 200 beats/min (to less than 40% of the control value) but the stimulation-induced ACh release did not exceed the ischemia-induced ACh release (Figs. 1 and 3). On the other hand, vagal stimulation that reduced the HR by only 10% produces a significant increase in the survival rate of chronic heart failure rats (Li et al. 2004). Therefore, vagal stimulation probably exerts its beneficial effects not only within the ischemic region but also outside of this region. For instance, vagal stimulation in dogs with a healed myocardial infarction is known to prevent lethal arrhythmia induced by exercise (Vanoli et al. 1991). Afferent vagal activation may also contribute to the cardioprotective effects. Further studies are clearly needed to identify the mechanisms underlying the vagally induced cardioprotective effects against myocardial infarction and chronic heart failure.

Conclusion

The present study demonstrated the presence of vagal innervation in the rabbit left ventricle. Acute myocardial ischemia significantly increased the myocardial interstitial ACh levels. In addition, a brief ischemic event (5 min) caused detectable increases in ACh levels, indicating that endogenous ACh release may provide a trigger for ischemic preconditioning.

Acknowledgments

This study was supported by the Health and Labour Sciences Research Grants (H18-nano-Ippan-003, H19-nano-Ippan-009, H20-katsudo-Shitei-007, and H21-nano-Ippan-005) from the Ministry of Health, Labour and Welfare of Japan; by a Grant-in-Aid for Scientific Research (No. 20390462) from the Ministry of Education, Culture, Sports, Science and Technology of Japan; and by the Industrial Technology Research Grant Program from the New Energy and Industrial Technology Development Organization (NEDO) of Japan.

References

Akiyama T, Yamazaki T, Ninomiya I. In vivo detection of endogenous acetylcholine release in cat ventricles. American Journal of Physiology 266 (3 Pt 2), H854–H860, 1994.

Brown OM. Cat heart acetylcholine: Structural proof and distribution. American Journal of Physiology 231 (3), 781–785, 1976.

Cason BA, Gamperl AK, Slocum RE, Hickey RF. Anesthetic-induced preconditioning: Previous administration of isoflurane decreases myocardial infarct size in rabbits. Anesthesiology 87 (5), 1182–1190, 1997.

Cohen MV, Liu GS, Downey JM. Preconditioning causes improved wall motion as well as smaller infarcts after transient coronary occlusion in rabbits. Circulation 84 (1), 341–349, 1991.

Glantz SA. Primer of Biostatistics, 5th ed. McGraw-Hill, New York, 2002.

Kawada T, Yamazaki T, Akiyama T, Sato T, Shishido T, Inagaki M, Takaki H, Sugimachi M, Sunagawa K. Differential acetylcholine release mechanisms in the ischemic and non-ischemic myocardium. Journal of Molecular and Cellular Cardiology 32 (3), 405–414, 2000.

Kawada T, Yamazaki T, Akiyama T, Shishido T, Inagaki M, Uemura K, Miyamoto T, Sugimachi M, Takaki H, Sunagawa K. In vivo assessment of acetylcholine releasing function at cardiac vagal nerve terminals. American Journal of Physiology. Heart and Circulatory Physiology 281 (1), H139–H145, 2001.

Kawada T, Yamazaki T, Akiyama T, Mori H, Inagaki M, Shishido T, Takaki H, Sugimachi M, Sunagawa K. Effects of brief ischaemia on myocardial acetylcholine and noradrenaline levels in anaesthetized cats. Autonomic Neuroscience: Basic and Clinical 95 (1–2), 37–42, 2002.

Kawada T, Yamazaki T, Akiyama T, Li M, Ariumi H, Mori H, Sunagawa K, Sugimachi M. Vagal stimulation suppresses ischemia-induced myocardial interstitial norepinephrine release. Life Sciences 78 (8), 882–887, 2006a.

Kawada T, Yamazaki T, Akiyama T, Uemura K, Kamiya A, Shishido T, Mori H, Sugimachi M. Effects of Ca^{2+} channel antagonists on nerve stimulation-induced and ischemia-induced myocardial interstitial acetylcholine release in cats. American Journal of Physiology. Heart and Circulatory Physiology 291 (5), H2187–H2191, 2006b.

Kawada T, Yamazaki T, Akiyama T, Shishido T, Shimizu S, Mizuno M, Mori H, Sugimachi M. Regional difference in ischaemia-induced myocardial interstitial noradrenaline and acetylcholine releases. Autonomic Neuroscience: Basic and Clinical 137 (1–2), 44–50, 2007.

Kawada T, Yamazaki T, Akiyama T, Kitagawa H, Shimizu S, Mizuno M, Li M, Sugimachi M. Vagal stimulation suppresses ischemia-induced myocardial interstitial myoglobin release. Life Sciences 83 (13–14), 490–495, 2008.

Kilbinger H, Löffelholz K. The isolated perfused chicken heart as a tool for studying acetylcholine output in the absence of cholinesterase inhibition. Journal of Neural Transmission 38, 9–14, 1976.

Kitagawa H, Yamazaki T, Akiyama T, Sugimachi M, Sunagawa K, Mori H. Microdialysis separately monitors myocardial interstitial myoglobin during ischemia and reperfusion. American Journal of Physiology Heart and Circulatory Physiology 289 (2), H924–H930, 2005.

Krieg T, Qin Q, Philipp S, Alexeyev MF, Cohen MV, Downey JM. Acetylcholine and bradykinin trigger preconditioning in the heart through a pathway that induces Akt and NOS. American Journal of Physiology. Heart and Circulatory Physiology 287 (6), H2606–H2611, 2004.

Li M, Zheng C, Sato T, Kawada T, Sugimachi M, Sunagawa K. Vagal nerve stimulation markedly improves long-term survival after chronic heart failure in rats. Circulation 109 (1), 120–124, 2004.

Liu GS, Thornton J, Van Winkle DM, Stanley AW, Olsson RA, Downey JM. Protection against infarction afforded by preconditioning is mediated by A_1 adenosine receptors in rabbit heart. Circulation 84 (1), 350–356, 1991.

Matsuura W, Sugimachi M, Kawada T, Sato T, Shishido T, Miyano H, Nakahara T, Ikeda Y, Alexander Jr J, Sunagawa K. Vagal stimulation decreases left ventricular contractility mainly through negative chronotropic effect. American Journal of Physiology 273 (2 Pt 2), H534–H539, 1997.

Murry CE, Jennings RB, Reimer KA. Preconditioning with ischemia: A delay of lethal cell injury in ischemic myocardium. Circulation 74 (5), 1124–1136, 1986.

Nakayama Y, Miyano H, Shishido T, Inagaki M, Kawada T, Sugimachi M, Sunagawa K. Heart rate-independent vagal effect on end-systolic elastance of the canine left ventricle under various levels of sympathetic tone. Circulation 104 (19), 2277–2279, 2001.

Piper HM, Abdallah Y, Schäfer C. The first minutes of reperfusion: A window of opportunity for cardioprotection. Cardiovascular Research 61 (3), 365–371, 2004.

Przyklenk K, Kloner RA. Low-dose iv acetylcholine acts as a "preconditioning-mimetic" in the canine model. Journal of Cardiac Surgery 10 (4), 389–395, 1995.

Qin Q, Downey JM, Cohen MV. Acetylcholine but not adenosine triggers preconditioning through PI3-kinase and a tyrosine kinase. American Journal of Physiology. Heart and Circulatory Physiology 284 (2), H727–H734, 2003.

Richard V, Blanc T, Kaeffer N, Tron C, Thuillez C. Myocardial and coronary endothelial protective effects of acetylcholine after myocardial ischaemia and reperfusion in rats: Role of nitric oxide. British Journal of Pharmacology 115 (8), 1532–1538, 1995.

Shimizu S, Akiyama T, Kawada T, Shishido T, Yamazaki T, Kamiya A, Mizuno M, Sano S, Sugimachi M. In vivo direct monitoring of vagal acetylcholine release to the sinoatrial node. Autonomic Neuroscience: Basic and Clinical 148 (1–2), 44–49, 2009.

Snedecor GW, Cochran WG. Statistical Methods. Iowa State, Iowa, pp. 290–291, 1989.

Ståhle L. The use of microdialysis in pharmacokinetics and pharmacodynamics. In: Robinson, TE, JusticeJr. Jr, JB (Eds.), Microdialysis in the Neurosciences, pp. 155–174. Elsevier Science Ltd. New York, 1991.

Thames MD, Klopfenstein HS, Abboud FM, Mark AL, Walker JL. Preferential distribution of inhibitory cardiac receptors with vagal afferents to the inferoposterior wall of the left ventricle activated during coronary occlusion in the dog. Circulation Research 43 (4), 512–519, 1978.

Uemura K, Li M, Tsutsumi T, Yamazaki T, Kawada T, Kamiya A, Inagaki M, Sunagawa K, Sugimachi M. Efferent vagal nerve stimulation induces tissue inhibitor of metalloproteinase-1 in myocardial ischemia–reperfusion injury in rabbit. American Journal of Physiology. Heart and Circulatory Physiology 293 (4), H2254–H2261, 2007.

Vanoli E, de Ferrari GM, Stramba-Badiale M, Hull Jr SS, Foreman RD, Schwartz PJ. Vagal stimulation and prevention of sudden death in conscious dogs with a healed myocardial infarction. Circulation Research 68 (5), 1471–1481, 1991.

Yao Z, Gross GJ. Acetylcholine mimics ischemic preconditioning via a glibenclamide-sensitive mechanism in dogs. American Journal of Physiology 264 (6 Pt 2), H2221–H2225, 1993.

Autonomic Neuroscience: Basic and Clinical 148 (2009) 44–49

Contents lists available at ScienceDirect

Autonomic Neuroscience: Basic and Clinical

journal homepage: www.elsevier.com/locate/autneu

In vivo direct monitoring of vagal acetylcholine release to the sinoatrial node

Shuji Shimizu [a,c,d,*], Tsuyoshi Akiyama [b], Toru Kawada [a], Toshiaki Shishido [a], Toji Yamazaki [b], Atsunori Kamiya [a], Masaki Mizuno [a], Shunji Sano [c], Masaru Sugimachi [a]

[a] Department of Cardiovascular Dynamics, Advanced Medical Engineering Center, National Cardiovascular Center Research Institute, Osaka, Japan
[b] Department of Cardiac Physiology, National Cardiovascular Center Research Institute, Osaka, Japan
[c] Department of Cardiovascular Surgery, Okayama University Graduate School of Medicine, Dentistry and Pharmaceutical Sciences, Okayama, Japan
[d] Japan Association for the Advancement of Medical Equipment, Tokyo, Japan

ARTICLE INFO

Article history:
Received 30 September 2008
Received in revised form 16 February 2009
Accepted 23 February 2009

Keywords:
Heart rate
Vagal nerve activity
Acetylcholine
Sinoatrial node
Right atrium
Microdialysis
Anesthetized rabbit

ABSTRACT

To directly monitor vagal acetylcholine (ACh) release into the sinoatrial node, which regulates heart rate, we implanted a microdialysis probe in the right atrium near the sinoatrial node and in the right ventricle of anesthetized rabbits, and perfused with Ringer's solution containing eserine. (1) Electrical stimulation of right or left cervical vagal nerve decreased atrial rate and increased dialysate ACh concentration in the right atrium in a frequency-dependent manner. Compared to left vagal stimulation, right vagal nerve stimulation decreased atrial rate to a greater extent at all frequencies, and increased dialysate ACh concentration to a greater extent at 10 and 20 Hz. However, dialysate ACh concentration in the right atrium correlated well with atrial rate independent of whether electrical stimulation was applied to the right or left vagal nerve (atrial rate $= 304 - 131 \times \log[\mathrm{ACh}]$, $R^2 = 0.77$). (2) Right or left vagal nerve stimulation at 20 Hz decreased atrial rate and increased dialysate ACh concentrations in both the right atrium (right, 17.9 ± 4.0 nM; left, 7.9 ± 1.4 nM) and right ventricle (right, 0.9 ± 0.3 nM; left, 1.0 ± 0.4 nM). However, atrial dialysate ACh concentrations were significantly higher than ventricular concentrations, while ventricular dialysate ACh concentrations were not significantly different between right and left vagal nerve stimulation. (3) The response of ACh release to right and left vagal nerve stimulation was abolished by intravenous administration of a ganglionic blocker, hexamethonium bromide. In conclusion, ACh concentration in dialysate from the right atrium, sampled by microdialysis, is a good marker of ACh release from postganglionic vagal nerves to the sinoatrial node.

1. Introduction

Parasympathetic nerves play an important role in the regulation of heart rate under physiological conditions. To better understand the parasympathetic control of heart rate, it is important to quantitatively assess the efferent cardiac vagal nerve activity. Several methods have been used to assess this activity. Efferent cardiac vagal nerve electrical activity has been measured directly at the preganglionic site in several studies (Jewett, 1964; Kunze, 1972). We have developed a microdialysis technique which is used with high-performance liquid chromatography (HPLC) to monitor in vivo endogenous acetylcholine (ACh) release in the heart (Akiyama et al., 1994). Using this technique, we were able to monitor endogenous ACh release into the ventricular myocardium (Akiyama et al., 1994; Kawada et al., 2001). This technique permits the estimation of relative changes in postganglionic efferent cardiac vagal nerve activity in the ventricle.

However, vagal innervation is known to be heterogeneous in the heart. Kilbinger and Löffelholz (1976) reported that the ACh content of the ventricle was 41% and 19% of the atrial content in chicken and rabbit, respectively. Brown (1976) reported that ACh concentration was higher in the atrium than the ventricle, and that ACh content was higher in the right than the left portions in both the atrium and ventricle of the cat. Thus, to better understand the parasympathetic control of heart rate, which is the sinus rate under physiological conditions, we need information about the activities of postganglionic vagal nerves innervating the sinoatrial (SA) node.

In this study, we developed a dialysis probe using shorter dialysis fiber, which was suitable for implantation into the atrium. Using this dialysis probe, we tried to monitor myocardial interstitial ACh levels in the right atrium, especially near the SA node. Furthermore, we investigated whether the myocardial interstitial ACh levels reflect relative changes in activity of postganglionic vagal nerves innervating the SA node.

2. Materials and methods

2.1. Surgical preparation

Animal care was provided in accordance with the *Guiding Principles for the Care and Use of Animals in the Field of Physiological Sciences*

* Corresponding author. Department of Cardiovascular Dynamics, Advanced Medical Engineering Center, National Cardiovascular Center Research Institute, 5-7-1, Fujishiro-dai, Suita, Osaka, 565-8565 Japan. Tel.: +81 6 6833 5012; fax: +81 6 6835 5403.
E-mail address: shujismz@ri.ncvc.go.jp (S. Shimizu).

1566-0702/$ – see front matter © 2009 Elsevier B.V. All rights reserved.
doi:10.1016/j.autneu.2009.02.006

approved by the Physiological Society of Japan. All protocols were approved by the Animal Subject Committee of the National Cardiovascular Center. Forty-three Japanese white rabbits weighing from 2.2 to 2.9 kg were anesthetized using an intravenous injection of pentobarbital sodium (50 mg/kg) via the marginal ear vein, followed by a continuous intravenous infusion of α-chloralose and urethane (16 mg/kg/h and 100 mg/kg/h) through a catheter inserted into the femoral vein to maintain an appropriate level of anesthesia. The animals were intubated and ventilated mechanically with room air mixed with oxygen. Systemic arterial pressure was monitored by a catheter inserted into the femoral artery. Esophageal temperature, which was measured by a thermometer (CTM-303, TERUMO, Japan), was maintained between 38 and 39 °C using a heating pad. In all protocols, bilateral vagal nerves were exposed through a midline cervical incision and sectioned at the neck after the control dialysate sampling. A pair of bipolar stainless steel electrodes was attached to the efferent side of the right or left vagal nerve. The nerve and electrode were covered with warmed mineral oil for insulation. When vagal stimulation was required, the efferent vagal nerve was stimulated by a digital stimulator (SEN-7203, Nihon Kohden, Japan). The pulse duration and amplitude of nerve stimulation were set at 1 ms and 10 V.

With the animal in the lateral position, right lateral thoracotomy was performed and the right 3rd to 5th ribs were partially resected to expose the heart. After incision of the pericardium, stainless steel wires were attached to the apex and the anterior wall of the left ventricle for ventricular pacing. To prevent severe bradycardia and cardiac arrest induced by vagal stimulation, left ventricular pacing was performed at the same frequency as the heart rate before vagal stimulation. The ventricular rate was determined from the electrocardiogram using a cardiotachometer. Another pair of stainless steel wires was attached to the appendage of the right atrium for recording atrial electrocardiogram, from which atrial rate was determined. Heparin sodium (100 IU/kg) was administered intravenously to prevent blood coagulation. At the end of the experiment, animals were killed with an overdose injection of pentobarbital sodium. A postmortem examination confirmed that the dialysate probe did not penetrate into the atrial or ventricular cavity and the dialysis membrane was positioned totally within the atrial or ventricular wall.

2.2. Dialysis technique

The materials and properties of the dialysis probe have been described previously (Akiyama et al., 1994). Briefly, we designed a handmade transverse dialysis probe. A dialysis fiber of semipermeable membrane (4 mm length, 310 μm outer diameter, 200 μm inner diameter; PAN-1200, 50,000 molecular weight cutoff; Asahi Chemical, Tokyo, Japan) was attached at both ends to polyethylene tubes (25 cm length, 500 μm outer diameter, 200 μm inner diameter). A fine guiding needle (30 mm length, 510 μm outer diameter, 250 μm inner diameter) with a stainless steel rod (5 mm length, 250 μm outer diameter) was used for the implantation of the dialysis probe. In protocol 1 and 3, a dialysis probe was implanted in the right atrium near the junction between the superior vena cava and the right atrium. In protocol 2, a dialysis probe was also implanted in the right ventricular free wall. After implantation, the dialysis probe was perfused with Ringer's solution (NaCl 147 mM, KCl 4 mM, $CaCl_2$ 3 mM) containing the cholinesterase inhibitor eserine (100 μM) at a speed of 2 μl/min, using a microinjection pump (CMA/100, Carnegie Medicin, Sweden). Experimental protocols were started 120 min after implantation of the dialysis probe. We took account of the dead space between the dialysis membrane and the sample tube at the start of each dialysate sampling. Phosphate buffer (4 μl) containing an internal standard (isopropylhomocholine chloride) was transferred into each sample tube before dialysate sampling. Dialysate sampling periods were set at 10 min (1 sample volume = 20 μl).

2.3. Analytic procedure

Dialysate ACh was assayed using HPLC with electrochemical detection. An autosampler (CMA/200, Carnegie Medicin) was used. The HPLC system consisted of a pump with a pulse dumper (EP-300, Eicom, Japan), a separation column (AC-Gel, styrene polymer, 4 μm particle size, 2 mm inner diameter × 150 mm length, Eicom), an immobilized enzyme column (AC-Enzymepack, 1 mm inner diameter × 4 mm length, Eicom), an electrochemical detector (ECD-300, Eicom), and a degasser (DG-300, Eicom). The electrochemical detector was operated with a platinum working electrode at + 0.45 V vs. an Ag/AgCl reference electrode. The mobile phase was 50 mM potassium bicarbonate solution containing 400 mg/L of sodium 1-decansulfonate and 50 mg/L of disodium–EDTA. The pump flow rate was 0.15 ml/min.

Chromatograms were recorded and analyzed by an analog-to-digital converter (Power Chrom EPC-300, AD Instruments, Australia) with a computer. Concentrations of ACh and isopropylhomocholine chloride were determined by measuring the peak areas. The absolute detection limit of ACh was 10 fmol/injection (signal-to-noise ratio = 3).

2.4. Experimental protocols

2.4.1. Protocol 1

To examine whether atrial dialysate ACh concentration reflects ACh release from cardiac vagal nerves, we investigated the relationship between the dialysate ACh concentration in the right atrium and the frequency of right and left vagal nerve stimulation. We sampled control dialysate before and after vagal transection. Then we stimulated the right ($n = 8$) or left ($n = 8$) efferent vagal nerves for 10 min at frequencies of 5, 10, 20 and 40 Hz, and sampled dialysate during each stimulation. Ten minutes after vagal nerve stimulation, we sampled the dialysate again to check the recovery of ACh levels.

2.4.2. Protocol 2

To investigate the difference in vagal innervation density between the right atrium and right ventricle, we compared the atrial and ventricular dialysate ACh concentrations under control condition and during electrical vagal nerve stimulation. Control dialysates were sampled after vagal transection. Then the right ($n = 5$) or left ($n = 5$) efferent vagal nerve was stimulated for 10 min at a frequency of 20 Hz, and dialysates were collected during vagal stimulation.

2.4.3. Protocol 3

ACh is released from both pre- and post-ganglionic vagal nerves as a primary neurotransmitter. The cardiac vagal nerve ganglia are localized near the atrium (Löffelholz and Pappano, 1985). Electrical stimulation of cervical vagal nerves activates the entire efferent parasympathetic pathway, including both preganglionic and postganglionic nerves in the atrium. Thus it is possible that pre- and/or post-ganglionic nerves serve as the source of dialysate ACh. To determine whether pre- or post-ganglionic nerves are the source of atrial dialysate ACh, we observed ACh release in response to nerve stimulation before and after blockade of ganglionic transmission. We sampled control dialysate after vagal transection. Then we stimulated the right ($n = 9$) or left ($n = 8$) vagal nerve at a frequency of 20 Hz before and after intravenous administration of hexamethonium bromide (30 mg/kg) and sampled dialysate during vagal stimulation. To prevent severe hypotension induced by hexamethonium, arterial pressure was maintained by continuous intravenous infusion of phenylephrine (17.2 ± 1.6 μg/kg/min).

2.5. Statistical analysis

All data are presented as mean ± SE. For each protocol, heart rate and mean arterial pressure were compared by one-way repeated measures analysis of variance followed by a Dunnett's test against

control (Glantz, 2005). In protocol 1, we compared vagal stimulation-induced ACh release among the seven groups by one-way repeated measures analysis of variance followed by Tukey's test. Heart rates (atrial rate) and dialysate ACh concentrations during right and left vagal stimulation were compared by unpaired *t*-test. After logarithmic transformation of atrial dialysate ACh concentration, a linear regression analysis was performed to examine the relation between dialysate ACh concentration and atrial rate. In protocol 2, we compared atrial and ventricular dialysate ACh concentrations during vagal stimulation by two-way repeated measures analysis of variance. We also compared the effects of right and left vagal stimulation on atrial and ventricular dialysate ACh concentrations using an unpaired *t*-test. In protocol 3, we compared stimulation-induced ACh release with and without hexamethonium using one-way repeated measures analysis of variance followed by a Dunnett's test against control. Differences were considered significant at $P<0.05$.

3. Results

3.1. Protocol 1

Responses of heart rate and mean arterial pressure to electrical vagal nerve stimulation are shown in Table 1. Transection of bilateral vagal nerves did not change heart rate or mean arterial pressure significantly. While both right and left vagal stimulation decreased heart rate in proportion to the frequency of the stimulus, right vagal nerve stimulation decreased the heart rate to a greater extent than left vagal nerve stimulation at all stimulus frequencies tested ($P<0.05$ at 5 Hz, $P<0.01$ at 10 Hz, $P<0.05$ at 20 Hz and $P<0.05$ at 40 Hz). Heart rate recovered to the pre-stimulation levels after stimulation. Both right and left vagal nerve stimulation with ventricular pacing decreased mean arterial pressure. Mean arterial pressure recovered partially but remained lower than the pre-stimulation levels 10 min after stimulation.

Transection of bilateral vagal nerves did not change dialysate ACh concentration (Fig. 1). Both right and left vagal stimulation increased the dialysate ACh concentration in proportion to the stimulus frequency. Right vagal stimulation increased the dialysate ACh concentration from 1.9 ± 0.3 nM in the post-transection control to 2.7 ± 0.4 nM at 5 Hz ($P<0.05$ vs. control), 5.5 ± 0.8 nM at 10 Hz ($P<0.01$ vs. 5 Hz), 17.2 ± 3.0 nM at 20 Hz ($P<0.01$ vs. 10 Hz) and 40.4 ± 8.4 nM at 40 Hz ($P<0.01$ vs. 20 Hz). Dialysate ACh concentration recovered to 2.2 ± 0.3 nM 10 min after stimulation. Left vagal stimulation increased dialysate ACh concentration from 1.6 ± 0.3 nM in the post-transection control to 2.2 ± 0.4 nM at 5 Hz ($P<0.05$ vs. control), 3.2 ± 0.5 nM at 10 Hz ($P<0.01$ vs. control), 8.2 ± 1.4 nM at 20 Hz ($P<0.01$ vs. 10 Hz) and 24.7 ± 4.6 nM at 40 Hz ($P<0.01$ vs. 20 Hz). Dialysate ACh concentration recovered to 2.0 ± 0.5 nM 10 min after stimulation. While both right and left vagal stimulation increased dialysate ACh concentration in a frequency-dependent manner, right vagal nerve stimulation increased dialysate ACh concentration to a greater extent than left vagal nerve stimulation at 10 and 20 Hz (N.S. at 5 Hz, $P<0.05$ at 10 Hz, $P<0.05$ at 20 Hz and N.S. at 40 Hz).

Table 1
Responses of heart rate and mean arterial pressure to electrical vagal nerve stimulation (protocol 1).

	Heart rate (bpm)	Mean arterial pressure (mm Hg)
Rt vagal stimulation ($n=8$)	Atrial rate (pacing rate)	
Control before transection	298 ± 8	83 ± 4
Control after transection	293 ± 7	85 ± 6
VNS (5 Hz)	$246\pm5^{**}$ (296 ± 5)	71 ± 7
VNS (10 Hz)	$201\pm6^{**}$ (296 ± 5)	77 ± 6
VNS (20 Hz)	$121\pm7^{**}$ (296 ± 5)	72 ± 8
VNS (40 Hz)	$88\pm4^{**}$ (296 ± 5)	$65\pm7^{**}$
After VNS	287 ± 10	70 ± 9
Lt vagal stimulation ($n=8$)	Atrial rate (pacing rate)	
Control before transection	305 ± 8	89 ± 4
Control after transection	308 ± 5	92 ± 6
VNS (5 Hz)	$267\pm6^{*}$ (309 ± 4)	$79\pm6^{**}$
VNS (10 Hz)	$236\pm10^{**}$ (309 ± 4)	82 ± 6
VNS (20 Hz)	$165\pm13^{**}$ (309 ± 4)	$77\pm5^{**}$
VNS (40 Hz)	$129\pm16^{**}$ (309 ± 4)	$67\pm6^{**}$
After VNS	305 ± 13	$75\pm8^{**}$

Values are means ± SE; *n*: numbers of rabbits; Rt: right; Lt: left; VNS: electrical vagal nerve stimulation; $^{**}P<0.01$ vs. control; $^{*}P<0.05$ vs. control.

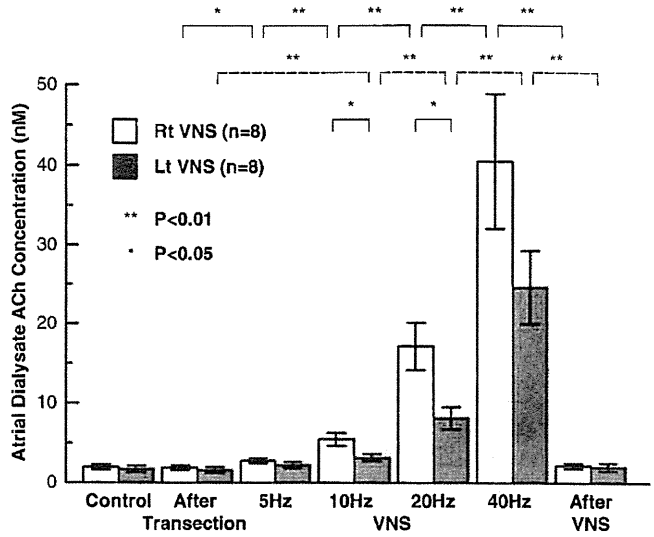

Fig. 1. Dialysate ACh concentrations of controls and during electrical vagal nerve stimulation at different frequencies. Right vagal nerve stimulation increased atrial dialysate ACh concentration from 1.9 ± 0.3 nM in the post-transection control to 2.7 ± 0.4 nM at 5 Hz, 5.5 ± 0.8 nM at 10 Hz, 17.2 ± 3.0 nM at 20 Hz and 40.4 ± 8.4 nM at 40 Hz. Left vagal nerve stimulation increased atrial dialysate ACh concentration from 1.6 ± 0.3 nM in the control to 2.2 ± 0.4 nM at 5 Hz, 3.2 ± 0.5 nM at 10 Hz, 8.2 ± 1.4 nM at 20 Hz and 24.7 ± 4.6 nM at 40 Hz. Values are means ± SE; Rt: right; Lt: left; VNS: electrical vagal nerve stimulation; *n*: number of rabbits: $^{**}P<0.01$, $^{*}P<0.05$.

The relationship between dialysate ACh concentration and atrial rate ($n=16$) is shown in Fig. 2. Dialysate ACh concentration in the right atrium correlated well with atrial rate (AR; $AR=304-131\times\log[ACh]$, $R^2=0.77$). There was no significant difference in the intercept or slope of regression line between right and left vagal nerve stimulation (right: $AR=304-135\times\log[ACh]$, $R^2=0.79$; left: $AR=303-126\times\log[ACh]$, $R^2=0.73$) (Glantz, 2005). The correlation between dialysate ACh concentration and atrial rate was independent of the side of vagal nerve stimulation.

3.2. Protocol 2

Responses of heart rate and mean arterial pressure were similar to the responses to vagal stimulation at 20 Hz in protocol 1 (Table 2). Responses of ACh release in the right atrium and right ventricle to vagal stimulation are shown in Fig. 3. Right vagal stimulation increased the atrial dialysate ACh concentration from 2.6 ± 0.6 nM in the post-transection control to 17.9 ± 4.0 nM ($P<0.01$) and the ventricular dialysate ACh concentration from 0.4 ± 0.2 nM to 0.9 ± 0.3 nM ($P<0.01$). Left vagal stimulation also increased the atrial dialysate ACh concentration from 1.5 ± 0.4 nM to 7.9 ± 1.4 nM ($P<0.01$) and the ventricular dialysate ACh concentration from 0.3 ± 0.1 nM in the control to 1.0 ± 0.4 nM ($P<0.01$). Atrial dialysate ACh concentrations were higher than ventricular dialysate ACh concentrations in both right and left vagal stimulation ($P<0.01$). The interaction between the stimulation and the position of probe (atrium or ventricle) was significant ($P<0.01$). There was no difference in ventricular dialysate ACh concentration between right and left vagal stimulation, but atrial dialysate ACh concentration was significantly

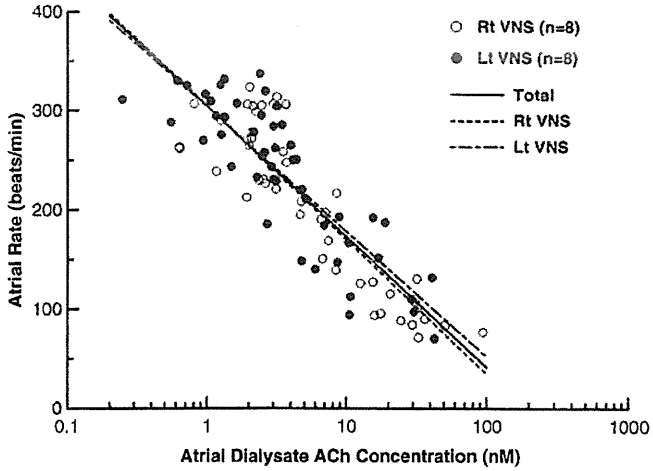

Fig. 2. Relation between dialysate ACh concentration (logarithmic scale) and atrial rate. Dialysate ACh concentration in the right atrium correlates well with atrial rate ($R^2=0.77$). Solid line, regression line fitting all 96 data points; dotted line, regression line fitting 48 data points of right vagal nerve stimulation; dot-dashed line, regression line fitting 48 data points of left vagal nerve stimulation. Rt: right; Lt: left; VNS: electrical vagal nerve stimulation.

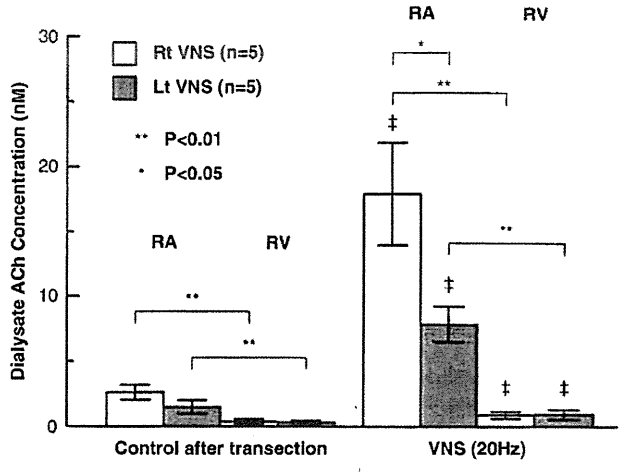

Fig. 3. Dialysate ACh concentrations in right atrium and right ventricle of controls and during electrical vagal nerve stimulation. Right vagal nerve stimulation significantly increased dialysate ACh concentration from 2.6±0.6 to 17.9±4.0 nM in the right atrium ($P<0.01$) and from 0.4±0.2 to 0.9±0.3 nM in the right ventricle ($P<0.01$). Left vagal nerve stimulation also increased dialysate ACh concentrations from 1.5±0.4 to 7.9±1.4 nM in the right atrium ($P<0.01$) and from 0.3±0.1 to 1.0±0.4 nM in the right ventricle ($P<0.01$). Dialysate ACh concentrations in the right atrium were significantly higher than those in the ventricle ($P<0.01$). Right vagal nerve stimulation increased atrial dialysate ACh concentration more than left vagal nerve stimulation ($P<0.05$). Values are means±SE; Rt: right; Lt: left; RA: right atrium; RV: right ventricle; VNS: electrical vagal nerve stimulation; *n*: number of rabbits; ‡$P<0.01$ vs. control; **$P<0.01$, *$P<0.05$.

higher during right vagal stimulation compared to left vagal stimulation ($P<0.05$).

3.3. Protocol 3

Responses of heart rate and mean arterial pressure are shown in Table 3. Both right and left vagal nerve stimulation decreased heart rate markedly before administration of hexamethonium. Administration of hexamethonium decreased heart rate significantly but mildly compared to control. Mean arterial pressure was maintained at pre-stimulation levels by continuous intravenous infusion of phenylephrine. After administration of hexamethonium, both right and left vagal nerve stimulation did not change the heart rate. Right vagal stimulation increased dialysate ACh concentration from 2.5±0.4 to 16.3±2.8 nM ($P<0.01$), but right vagal stimulation after administration of hexamethonium failed to increase ACh concentration (2.2±0.4 nM) compared to control. Likewise, left vagal stimulation increased dialysate ACh concentration from 1.5±0.3 to 8.7±1.4 nM ($P<0.01$), but left vagal stimulation after administration of hexamethonium did not increase ACh concentration (1.5±0.3 nM) compared to control (Fig. 4).

4. Discussion

We demonstrated that the microdialysis technique permitted in vivo monitoring of ACh release into the sinoatrial node from postganglionic cardiac vagal nerves. Dialysate ACh concentration in the right atrium correlated well with atrial rate and this correlation was independent of the side of vagal stimulation. These results indicate that in vivo monitoring of the myocardial interstitial ACh levels in the right atrium by microdialysis provides a useful strategy to obtain insights into the physiological roles of the vagal system in regulating heart rate.

4.1. Characteristics of atrial dialysate ACh concentration

With both right and left vagal nerve stimulation, the dialysate ACh concentration in the right atrium increased with increasing stimulus frequency and decreased to prestimulation levels after stimulation (Fig. 1). These results indicate that atrial dialysate ACh reflects ACh release from cardiac vagal nerves innervating the right atrium. Right vagal nerve stimulation decreased the atrial rate more than left stimulation at all stimulus frequencies, and right vagal nerve stimulation increased dialysate ACh concentration more than left stimulation at 10- and 20-Hz. The right atrium, including the SA node, is innervated not only by the right but also by the left vagal nerve. Ardell and Randall (1986) reported that supramaximal right and left

Table 2
Responses of heart rate and mean arterial pressure to electrical vagal nerve stimulation (protocol 2).

	Heart rate (bpm)	Mean arterial pressure (mm Hg)
Rt vagal stimulation ($n=5$)	Atrial rate (pacing rate)	
Control after transaction	305±3	74±8
VNS (20 Hz)	122±4** (304±4)	65±9*
Control after VNS	300±3	68±8
Lt vagal stimulation ($n=5$)	Atrial rate (pacing rate)	
Control after transaction	306±5	95±3
VNS (20 Hz)	168±19** (308±5)	83±1**
Control after VNS	316±8	82±2**

Values are means±SE; *n*, numbers of rabbits; Rt: right; Lt: left; VNS: electrical vagal nerve stimulation; **$P<0.01$ vs. control; *$P<0.05$ vs. control.

Table 3
Responses of heart rate and mean arterial pressure to electrical vagal nerve stimulation (protocol 3).

	Heart rate (bpm)	Mean arterial pressure (mm Hg)
Rt vagal stimulation ($n=9$)	Atrial rate (pacing rate)	
Control after transaction	292±9	70±8
VNS (20 Hz)	116±7** (299±5)	69±7
Hexamethonium iv	257±4**	84±7*
VNS after hexamethonium iv	257±4**	83±8*
Lt vagal stimulation ($n=8$)	Atrial rate (pacing rate)	
Control after transaction	317±3	79±3
VNS (20 Hz)	173±13** (313±4)	81±3
Hexamethonium iv	273±4**	87±5
VNS after hexamethonium iv	273±4**	87±4

Values are means±SE; *n*, numbers of rabbits; Rt: right; Lt: left; VNS: electrical vagal nerve stimulation; iv: intravenous administration; **$P<0.01$ vs. control; *$P<0.05$ vs. control.

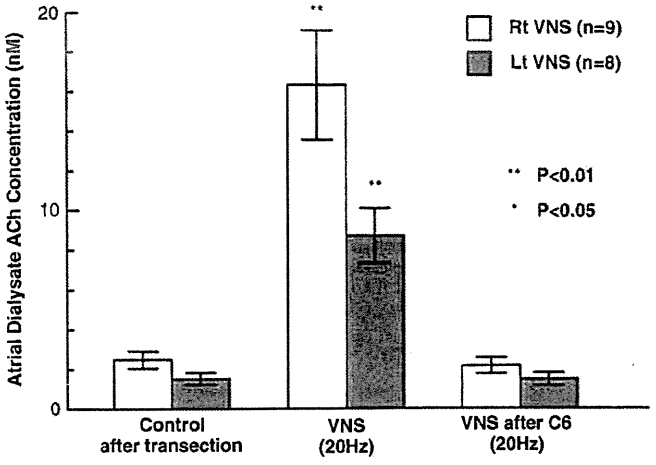

Fig. 4. Influence of ganglionic blocker on vagal nerve stimulation-induced ACh release. Right vagal nerve stimulation significantly increased atrial dialysate ACh concentration from 2.5±0.4 to 16.3±2.8 ($P<0.01$), and intravenous administration of hexamethonium suppressed the ACh concentration to 2.2±0.4 nM. Left vagal stimulation increased atrial dialysate ACh concentration from 1.5±0.3 to 8.7±1.4 nM ($P<0.01$), and hexamethonium suppressed the ACh concentration to 1.5±0.3 nM. Values are means±SE; Rt: right; Lt: left; VNS: electrical vagal nerve stimulation; C6: hexamethonium bromide; *n*: number of rabbits; **P<0.01 vs. control; *P<0.05 vs. control.

cervical vagal stimulation decreased the atrial rates to 16.3% and 48.7%, respectively, of prestimulation rates in dogs. In our study, right and left vagal stimulation at a frequency of 40 Hz also decreased the atrial rate to 30% and 42% of prestimulation rates. The difference in atrial rate response between right and left vagal nerve stimulation could be explained by the different innervation densities of the right and left vagal nerves in the right atrium including the SA node. The SA node is innervated by both right and left vagal nerves with a predominance of right vagal nerves (Ardell and Randall, 1986; Randall et al., 1985), and the response of atrial rate to vagal nerve stimulation could be ascribed to vagal ACh release into the SA node. The SA node is probably regulated by ACh released from the left as well as the right vagal nerves. In this study, dialysate ACh concentration in the right atrium (logarithmically transformed) correlated well with atrial rate, and this correlation was independent of right or left vagal stimulation (Fig. 2). These results suggest that dialysate ACh in the right atrium reflects ACh released into the SA node independent of whether the ACh originates from the right or left vagal nerves.

4.2. ACh release in atrium and ventricle

In this study, the mean dialysate ACh concentration in the right ventricle after transection of bilateral vagal nerves was 20 to 30% of that in the right atrium. During vagal nerve stimulation at 20 Hz, the atrial dialysate ACh concentration increased 5 to 7 times the control value but the ventricular dialysate ACh concentration increased to only 2 to 3 times the control value (Fig. 3). This difference between atrial and ventricular dialysate ACh concentrations could be related to the density of vagal innervation. These results are consistent with previous *in vitro* studies (Kilbinger and Löffelholz, 1976; Brown, 1976; Stanley et al., 1978). Kent et al. (1974) reported that the atrial myocardium of the vertebrate heart was richly innervated as identified by specific histochemical staining of acetylcholinesterase, in contrast to the scant innervation in the ventricular myocardium.

Right vagal nerve stimulation increased atrial dialysate ACh more than left stimulation. On the other hand, there was no difference in ventricular dialysate ACh concentration between right and left vagal nerve stimulation. Although the right atrium is predominantly innervated by the right vagal nerves, the right ventricle could be equally innervated by the right and left vagal nerves. When the right vagal nerve was stimulated at 20 Hz, heart rate decreased from 305±3 to 122±4 bpm. When the left vagal nerve was stimulated at 20 Hz, heart rate decreased from 306±5 to 169±19 bpm. This difference in heart rate response could be ascribed to vagal ACh release into the SA node. Atrial dialysate ACh concentrations were 17.9±4.0 and 7.9±1.4 nM ($P<0.05$) during stimulation of right and left vagal nerves, respectively. In contrast, there was no significant difference in ventricular dialysate ACh concentration between right and left vagal nerve stimulation. Therefore, we consider that dialysate ACh concentration in the right atrium may be a better index of ACh release into the SA node than dialysate ACh in the right ventricle.

4.3. Source of atrial dialysate ACh

In a previous study with anesthetized cats, we demonstrated that ACh in the dialysate sampled from left ventricular myocardium primarily reflects ACh released from postganglionic cardiac vagal nerves (Akiyama et al., 1994). Cardiac ganglia are located predominantly in the posterior aspect of the atria within the subepicardial connective tissue (Löffelholz and Pappano, 1985). It is possible that ACh released from stimulated preganglionic nerves contributes to ACh in the dialysate sampled from the right atrium. In this study, intravenous administration of hexamethonium bromide, a nicotinic antagonist, abolished the increase in ACh release during efferent vagal nerve stimulation. This result demonstrates that ACh in the dialysate sampled from the right atrium primarily originates from the postganglionic cardiac nerve endings.

4.4. Significance of monitoring ACh release to the SA node

Several studies have directly measured electrical efferent vagal nerve activities at the preganglionic site in vivo (Jewett, 1964; Kunze, 1972). Although this method has been used to estimate the net activity of cardiac vagal nerves, it is technically difficult to selectively measure the electrical activity of postganglionic vagal nerves innervating the SA node. Moreover, it is possible that preganglionic signals are modulated at intracardiac ganglionic sites (Gray et al., 2004). In fact, Bibevski and Dunlap (1999) have reported that attenuated vagal control in heart failure can be ascribed to attenuated ganglionic transmission. Therefore, information about postganglionic vagal nerve activity is important for understanding vagal control of heart rate.

4.5. Methodological consideration

First, we sectioned the vagi in the neck region but the sympathetic nerves were almost intact because the sympathetic nerves run separately from the vagi at the neck in rabbits. ACh released from vagal nerve terminals may interact with muscarinic receptors on postganglionic sympathetic nerve terminals to inhibit norepinephrine release prejunctionally (Levy, 1984).

Second, ACh is degraded by ACh esterase immediately after its release. Therefore to detect ACh release in vivo, addition of a specific ACh esterase inhibitor eserine into the perfusate is necessary. We used eserine at a concentration 10–100 times higher than that required in *in vitro* experimental settings because distribution of eserine across the semipermeable membrane is required, based on previous results (Akiyama et al., 1994). Eserine should spread around the semipermeable membrane, thereby affecting the ACh release in the vicinity of the dialysis membrane. Eserine may have increased the ACh level in the synaptic cleft and enhanced heart rate response by nerve stimulation, and may have also activated regulatory pathways such as autoinhibition of ACh release via muscarinic receptors.

5. Conclusion

We were able to monitor myocardial interstitial ACh levels in the right atrium around the SA node using a microdialysis technique.

Myocardial interstitial ACh level in the right atrium correlates well with atrial rate. Microdialysis combined with HPLC will become a powerful tool for understanding the parasympathetic control of heart rate.

Acknowledgements

This study was supported by Grants-in-Aid for scientific research (No. 19591829 and 20390462) from the Ministry of Education, Culture, Sports, Science and Technology; by Health and Labor Sciences Research Grants (H18-Iryo-Ippan-023, H18-nano-Ippan-003, H19-nano-Ippan-009 and H20-katsudo-Shitei-007) from the Ministry of Health, Labour and Welfare of Japan; and by the Industrial Technology Research Grant Program from New Energy and Industrial Technology Development Organization of Japan.

References

Akiyama, T., Yamazaki, T., Ninomiya, I., 1994. In vivo detection of endogenous acetylcholine release in cat ventricles. Am. J. Physiol. 266, H854–860.

Ardell, J.L., Randall, W.C., 1986. Selective vagal innervation of sinoatrial and atrioventricular nodes in canine heart. Am. J. Physiol. 251, H764–773.

Bibevski, S., Dunlap, M.E., 1999. Ganglionic mechanisms contribute to diminished vagal control in heart failure. Circulation 99, 2958–2963.

Brown, O.M., 1976. Cat heart acetylcholine: structural proof and distribution. Am. J. Physiol. 231, 781–785.

Glantz, S.A., 2005. Primer of Biostatistics, 6th ed. McGraw-Hill, New York.

Gray, A.L., Johnson, T.A., Ardell, J.L., Massari, V.J., 2004. Parasympathetic control of the heart. II. A novel interganglionic intrinsic cardiac circuit mediates neural control of heart rate. J. Appl. Physiol. 96, 2273–2278.

Jewett, D.L., 1964. Activity of single efferent fibres in the cervical vagus nerve of the dog, with special reference to possible cardio-inhibitory fibres. J. Physiol. 175, 321–357.

Kawada, T., Yamazaki, T., Akiyama, T., Shishido, T., Inagaki, M., Uemura, K., Miyamoto, T., Sugimachi, M., Takaki, H., Sunagawa, K., 2001. In vivo assessment of acetylcholine-releasing function at cardiac vagal nerve terminals. Am. J. Physiol. Heart Circ. Physiol. 281, H139–145.

Kent, K.M., Epstein, S.E., Cooper, T., Jacobowitz, D.M., 1974. Cholinergic innervation of the canine and human ventricular conducting system. Anatomic and electrophysiologic correlations. Circulation. 50, 948–955.

Kilbinger, H., Löffelholz, K., 1976. The isolated perfused chicken heart as a tool for studying acetylcholine output in the absence of cholinesterase inhibition. J. Neural Transm. 38, 9–14.

Kunze, D.L., 1972. Reflex discharge patterns of cardiac vagal efferent fibres. J. Physiol. 222, 1–15.

Levy, M.N., 1984. Cardiac sympathetic–parasympathetic interactions. Fed. Proc. 43, 2598–2602.

Löffelholz, K., Pappano, A.J., 1985. The parasympathetic neuroeffector junction of the heart. Pharmacol. Rev. 37, 1–24.

Randall, W.C., Ardell, J.L., Becker, D.M., 1985. Differential responses accompanying sequential stimulation and ablation of vagal branches to dog heart. Am. J. Physiol. 249, H133–140.

Stanley, R.L., Conaster, J., Dettbarn, W.D., 1978. Acetylcholine, choline acetyltransferase and cholinesterases in the rat heart. Biochem. Pharmacol. 27, 2409–2411.

Circ J 2009; **73:** 1395–1396

Coronary Artery Volume Noninvasively Measured With Multislice Computed Tomography

— Definition, Accuracy and Implication —

Masaru Sugimachi, MD; Toru Kawada, MD

In this issue of *Circulation Journal*, Ehara et al[1] describe a new concept of measuring 'coronary artery volume' (CAV) to examine the balance between coronary vasculature and myocardial mass. They have developed a method of measuring CAV as accurately as possible using 64-slice computed tomography (64-MSCT). An adaptive threshold value was used to detect the coronary artery border to improve the accuracy of CAV. Ehara et al have exemplified the usefulness of CAV by examining the relationship between CAV and left ventricular mass (LVM) in consecutive patients undergoing MSCT without significant coronary artery stenosis or left ventricular wall motion abnormality. The authors concluded that CAV increases with LVM, but that the increase was not sufficient for the increase in LVM.

Article p 1448

What is CAV?

The authors have defined CAV as the sum of the small volumes opacified by the contrast medium. The opacified small volumes were detected by the difference of radiodensity or Hounsfield unit (an index showing the degree of transparency to X-ray) using 64-MSCT (see below for details). Because the authors have analyzed data of routine 64-MSCT for the evaluation of coronary artery disease, the image is taken when the arterial side is mainly opacified, during the diastolic cardiac phase, and under coronary vasodilatation. Therefore, CAV mainly represents the sum of volumes of epicardial coronary arteries larger than the arteries undetectable due to the limited resolution of MSCT (see below).

How Accurate and Reproducible is CAV Measurement?

In this article, the authors have established a method of measuring CAV with every attempt to improve the accuracy and reproducibility for their MSCT device. These procedures are worthy of being discussed for other researchers who are interested in and would like to reproduce CAV measurement.

Inaccuracies and variability of CAV measurement would arise from (1) an arbitrary cut-off value for border detection, (2) partial volume effect, (3) motion artifact and (4) possible variable resolution of various MSCT devices. The authors have wisely minimized the errors introduced by the first 3 factors.

It is usually difficult to determine the border of the coronary arteries with a reasonable criterion. This may be because opacification of arteries is incomplete, or the opacification is thinner near the border than the center, resulting in a gradual decrease in radiodensity at the border, rather than a clear-cut abrupt change in radiodensity. In addition, at the border of small arteries, a voxel (the smallest size identified by 64-MSCT) may contain both arterial lumen (which is opacified) and arterial wall (which is not opacified). A voxel has a radiodensity of an intermediate value between an opacified and unopacified voxel, which is known as the 'partial volume effect'.

To minimize the errors introduced by an arbitrary cut-off value and the partial volume effect, the authors have developed a way of reasonably determining the cut-off value for border detection, based on preliminary phantom experiments with moving cylinders containing various concentrations of contrast medium. The results of these preliminary experiments are summarized in Figures 1–3 in Ehara et al! Figure 2 clearly shows that a cut-off value that exactly reproduces the phantom cylinder volume can be determined. The cut-off value is, however, not fixed, but changes with the true radiodensity of the contrast medium in the cylinder. Based on this, the authors determined the cut-off value for CAV measurement, adaptively in each subject, in reference to the radiodensity of the proximal region of the left and right coronary arteries. The cut-off value was not relatively influenced by different heart rates, which also decreased the degree of error by motion artifacts. Similar procedures may be applicable to quantitative coronary angiography.

The determined threshold is, however, only valid for the specific MSCT device used in the study by Ehara et al! If other researchers are to reproduce their CAV measurement, another attempt to determine the threshold for their device is necessary.

The limited resolution of MSCT would determine the definition of CAV. The authors used MSCT with an isotropic resolution of 400μm. This indicates that CAV in the paper by Ehara et al would be the sum of volume of the arteries >400μm. If MSCT is used with a different resolution, the definition of CAV would be different and CAV would be systematically different.

(Received June 17, 2009; accepted June 17, 2009)
Department of Cardiovascular Dynamics, Advanced Medical Engineering Center, National Cardiovascular Center Research Institute, Suita, Japan
Mailing address: Masaru Sugimachi, MD, Department of Cardiovascular Dynamics, Advanced Medical Engineering Center, National Cardiovascular Center Research Institute, 5-7-1 Fujishirodai, Suita 565-8565, Japan. E-mail: su91mach@ri.ncvc.go.jp

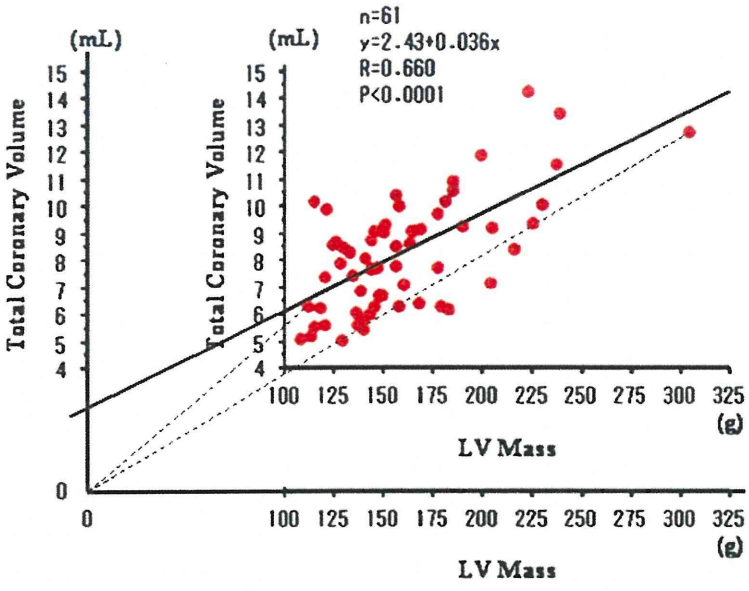

Figure. Linear regression between coronary artery volume (total coronary volume) and left ventricular (LV) mass (reproduced and modified from Ehara et al[1]). The axes are extended and the regression line is extrapolated to show a positive offset of coronary artery volume. Schematically, the authors have compared the slopes of dashed lines.

Is CAV a Proxy for Capillary Density or Coronary Flow Reserve?

The relation between coronary vasculature and myocardial mass, or more specifically inappropriate perfusion of the myocardium, has been traditionally examined histologically[2] by capillary density. Later, similar information was obtained in vivo by the measurement of coronary flow reserve. In fact, some have described the relationship between coronary capillary density and coronary flow reserve in patients with hypertrophic cardiomyopathy[3] in patients with idiopathic dilated cardiomyopathy[4] or in mini pigs with hypercholesterolemia[5]

In contrast, the way in which CAV correlates with coronary capillary density or coronary flow reserve is yet to be determined. As CAV measures the volume of arteries far larger than capillaries, these problems need to be resolved (eg, by animal experiments) before we can measure CAV in patients with a wide variety of cardiovascular diseases.

It is also reasonable to assume CAV may provide information other than coronary capillary density or coronary flow reserve. In Ehara et al, CAV is only measured under nitroglycerine. The response of CAV to increased coronary flow or to endothelium-dependent vasodilatation may be of clinical value. If better accuracy and reproducibility is established, CAV may potentially replace quantitative coronary angiography for this purpose because of its noninvasive nature.

Is CAV Really Unmatched With LVM?

The authors' conclusion of unmatched CAV with LVM should be discussed. **Figure** shows the linear regression between CAV and LVM reproduced and modified from Figure 6 of Ehara et al. The modified figure has extended axes and the extrapolated regression line has been added.

Even though there is only a single data set for each patient, the authors assumed that the line started at the origin and calculated the slope. Schematically, they have compared the slopes of dashed lines.

Figure, however, indicates that the CAV–LVM relationship obtained from pooled data has a positive CAV offset, but does note indicate that the slope is shallow. Because there is no reason to deny the presence of a positive CAV offset, and because the slope was not compared with a standard slope, the conclusion of unmatched CAV with LVM is not solid.

This question may be resolved by comparing the CAV–LVM relationship obtained by sequential CAV measurement during physiological growth and that obtained during the progression of pathological hypertrophy of the heart in animal experiments.

Advantage of CAV Measurement

The noninvasive nature of CAV measurement enhances its clinical usefulness because it enables sequential evaluation and may help to bring evaluations still in the investigational stage into routine bedside practice. Similar technological developments (eg, coronary flow reserve by cine magnetic resonance[6]) may be combined and eventually enable the detailed pathophysiology of cardiovascular disease to be described.

References

1. Ehara S, Okuyama T, Shirai N, Sugioka K, Oe H, Itoh T, et al. Inadequate increase in the volume of major epicardial coronary arteries compared with that in left ventricular mass: Novel concept for characterization of coronary arteries using 64-slice computed tomography. *Circ J* 2009; **73:** 1448–1453.
2. Tomanek RJ, Wessel TJ, Harrison DG. Capillary growth and geometry during long-term hypertension and myocardial hypertrophy in dogs. *Am J Physiol* 1991; **261:** H1011–H1018.
3. Krams R, Kofflard MJ, Duncker DJ, Von Birgelen C, Carlier S, Kliffen M, et al. Decreased coronary flow reserve in hypertrophic cardiomyopathy is related to remodeling of the coronary microcirculation. *Circulation* 1998; **97:** 230–233.
4. Tsagalou EP, Anastasiou-Nana M, Agapitos E, Gika A, Drakos SG, Terrovitis JV, et al. Depressed coronary flow reserve is associated with decreased myocardial capillary density in patients with heart failure due to idiopathic dilated cardiomyopathy. *J Am Coll Cardiol* 2008; **52:** 1391–1398.
5. Theilmeier G, Verhamme P, Dymarkowski S, Beck H, Bernar H, Lox M, et al. Hypercholesterolemia in minipigs impairs left ventricular response to stress: Association with decreased coronary flow reserve and reduced capillary density. *Circulation* 2002; **106:** 1140–1146.
6. Sakuma H, Koskenvuo JW, Niemi P, Kawada N, Toikka JO, Knuuti J, et al. Assessment of coronary flow reserve using fast velocity-encoded cine MR imaging: Validation study using positron emission tomography. *Am J Roentgenol* 2000; **175:** 1029–1033.

31st Annual International Conference of the IEEE EMBS
Minneapolis, Minnesota, USA, September 2-6, 2009

Feedback Control of Multiple Hemodynamic Variables with Multiple Cardiovascular Drugs

Masaru Sugimachi, *Member, IEEE*, Kazunori Uemura,
Atsunori Kamiya, Shuji Shimizu, Masashi Inagaki, and Toshiaki Shishido

Abstract— **The ultimate goal of disease treatment is to control the biological system beyond the native regulation to combat pathological process. To maximize the advantage of drugs, we attempted to pharmacologically control the biological system at will, e.g., control multiple hemodynamic variables with multiple cardiovascular drugs. A comprehensive physiological cardiovascular model enabled us to evaluate cardiovascular properties (pump function, vascular resistance, and blood volume) and the feedback control of these properties. In 12 dogs, with dobutamine (5±3 $\mu g \cdot kg^{-1} \cdot min^{-1}$), nitroprusside (4±2 $\mu g \cdot kg^{-1} \cdot min^{-1}$), dextran (2±2 $ml \cdot kg^{-1}$), and furosemide (10 mg in one, 20 mg in one), rapid, sufficient and stable control of pump function, vascular resistance and blood volume resulted in similarly quick and stable control of blood pressure, cardiac output and left atrial pressure in 5±7, 7±5, and 12±10 minutes, respectively. These variables remained stable for 60 minutes (RMS 4±3 mmHg, 5±2 $ml \cdot min^{-1} \cdot kg^{-1}$, 0.8±0.6 mmHg, respectively).**

I. Introduction

THE ultimate goal of disease treatment is to control the biological system beyond the native regulation to combat pathological process. This control may be partly achieved by native regulatory systems, but these frequently fail when disease progresses.

Many pharmacological treatments have provided us with control measures that may act in ways not possible by native regulators. To fully take advantage of these medicines, we must establish ways of using these agents to control the biological system at our will. As an example, we tried to control multiple hemodynamic variables with multiple cardiovascular drugs.

Several closed-loop systems have succeeded in directly controlling a single hemodynamic variable [1,2]. Multiple-variable control, however, has been unsuccessful [3-5].

Multiple-input multiple-output feedback control remains a challenge if the input-output relationships for all combinations are of equal significance. We therefore tried to decouple the input-output relationships by using a comprehensive physiological cardiovascular model. The model enabled us to define a set of parallel independent relationships between cardiovascular properties and drugs: pump function / inotrope, vascular resistance / vasodilator, and blood volume / volume expander. The model also provided us with a method to quantitatively calculate cardiovascular properties.

Manuscript received April 7, 2009. This work was supported in part by Grant-in-Aid for Scientific Research (B 20300164, C 20500404) from the Ministry of Education, Culture, Sports, Science and Technology, by Health and Labour Sciences Research Grants (H19-nano-ippan-009, H20-katsudo -shitei-007) from the Ministry of Health, Labour and Welfare of Japan.

M. Sugimachi, K. Uemura, A. Kamiya, S. Shimizu, M. Inagaki, and T. Shishido are with the National Cardiovascular Center Research Institute, Suita, Osaka 5658565, Japan (corresponding author Masaru Sugimachi to provide phone: +81-6-6833-512; fax: +81-6-6835-5403; e-mail: su91mach@ri.ncvc.go.jp).

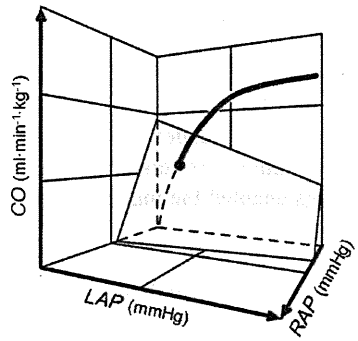

Fig. 1. Extended Guyton's model.
Thick curve, pump function of left and right heart; shaded surface, capacitive function of total vascular beds; CO, cardiac output; LAP, left atrial pressure; RAP, right atrial pressure.

II. Model and Methods

A. Cardiovascular property identification

Abnormalities of hemodynamic variables arise from abnormalities of cardiovascular properties, including pump function, vascular resistance, and blood volume. We identified these properties using an extended version of Guyton's circulatory equilibrium framework (Fig. 1) [6,7].

Pump function of the left heart (S_L) can be quantified as the ratio of cardiac output (CO) to the logarithm of left atrial pressure (LAP) ($S_L = CO / [\ln (LAP - 2.03) + 0.80]$). Systemic vascular resistance (R) can be calculated as blood pressure (BP) minus right atrial pressure (RAP) divided by CO. Stressed total blood volume (V) is obtained by $V = (CO + 19.61\ RAP + 3.49\ LAP) \times 0.129$.

B. Autopilot System

Autopilot controller of multiple hemodynamic variables consisted of multiple feedback loops. We designed these

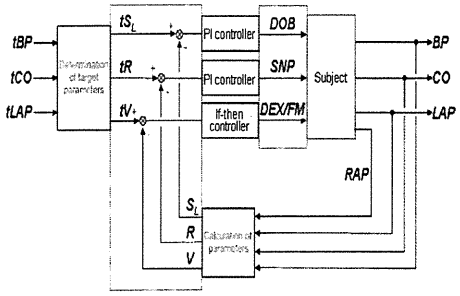

Fig. 2. Autopilot controller.
Calculated cardiovascular properties, rather than hemodynamic variables, were feedback-controlled to achieve multiple independent control of variables.

feedbacks as being independent of each other. The selection and the combination of controlled property and the controlling drugs enabled the independent operation (Fig. 2) [8].

S_L and R were controlled by proportional-integral (PI) feedback, with infusion of dobutamine (DOB) and sodium nitroprusside (SNP), respectively. Proportional and integral gain values were calculated using Chien-Hrones-Reswick's method [9] from gain, time constant, and dead-time delay of the approximated first-order step responses of S_L to DOB and R to SNP. We infused 10% dextran 40 solution (DEX, 10 $ml \cdot min^{-1}$) as long as V was <1 $ml \cdot kg^{-1}$ than the target, and injected furosemide (FM, 10 mg) every 20 minutes while V was >2 $ml \cdot kg^{-1}$ than the target.

C. *Animal Experiments*

We evaluated the performance of the autopilot controller in 12 adult anesthetized mongrel dogs (both sexes, 25±4 kg). We measured BP, CO, LAP and RAP. DOB, SNP, and DEX were automatically administered into the femoral vein through independent infusion routes, using either a computer-controlled roller pump or an infusion pump. FM was given through the jugular vein manually according to computer instructions.

These dogs underwent coronary microembolization, resulting in left ventricular failure. After hemodynamic stabilization, we began implementing control using the autopilot system.

III. Results

	Proportional gain (K_p) $\mu g \cdot ml^{-1}$	Integral gain (K_i) sec^{-1}
S_L control	0.06	0.01
R control	-1.37	0.007

Table 1. Selected gain parameters for designed controller.
Dose ($\mu g \cdot kg^{-1} \cdot min^{-1}$) of drugs for the control of S_L (DOB) or R (SNP) is determined as (Dose) = $K_p(1 + K_i / s)\,\Delta$(Controlled variable)

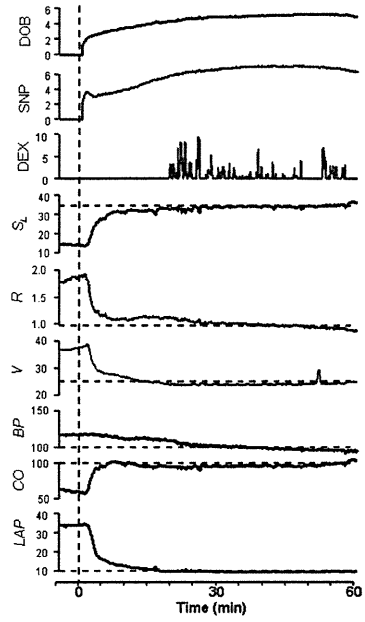

Fig. 3. An example of the automatic control of hemodynamics.
Feedback control was rapid, sufficient, and stable. DOB, dobutamine ($\mu g \cdot kg^{-1} \cdot min^{-1}$); SNP, sodium nitroprusside ($\mu g \cdot kg^{-1} \cdot min^{-1}$); DEX, dextran 40 solution ($ml \cdot min^{-1}$); S_L, pump function ($ml \cdot kg^{-1} \cdot min^{-1}$); R, resistance ($mmHg \cdot ml^{-1} \cdot kg \cdot min$); V, blood volume ($ml \cdot kg^{-1}$); BP, blood pressure (mmHg); CO, cardiac output ($ml \cdot kg^{-1} \cdot min^{-1}$); LAP, left atrial pressure (mmHg)

Based on the step response from coronary microembolized dogs, we determined the proportional and integral gain as shown in Table 1.

Similar to the example shown in Figure 3, in 12 dogs, by administering DOB (5±3 $\mu g \cdot kg^{-1} \cdot min^{-1}$), SNP (4±2 $\mu g \cdot kg^{-1} \cdot min^{-1}$), DEX (2±2 $ml \cdot kg^{-1}$), and FM (10 mg in one, 20 mg in one), rapid, sufficient and stable control of S_L, R and V. This resulted in corresponding appropriate control of BP, CO and LAP in 5±7, 7±5, and 12±10 minutes, respectively. These remained stable for 60 minutes (RMS BP=4±3 mmHg, CO=5±2 $ml \cdot min^{-1} \cdot kg^{-1}$, LAP=0.8±0.6 mmHg).

IV. Discussion

We have shown that by evaluating cardiovascular properties (pump function, vascular resistance, and blood volume), and then controlling these properties with individually selected drugs, we were able to automatically control multiple hemodynamic abnormalities rapidly, stably, and simultaneously.

Direct control of multiple hemodynamic variables, however, likely fails because each drug affects more than one variable. Direct control remains unfeasible even with more complicated methods developed in control engineering; appropriate physiological modeling and precise evaluation of cardiovascular properties are essential to achieving adequate control.

V. CONCLUSION

Calculating cardiovascular properties (pump function, vascular resistance, and blood volume) based on a comprehensive cardiovascular model and feedback control of these properties are required for the accurate control of multiple hemodynamic variables (BP, CO, LAP).

REFERENCES

[1] W. R. Chitwood, Jr, D. M. Cosgrove III, R. M. Lust, "Multicenter trial of automated nitroprusside infusion for postoperative hypertension. Titrator Multicenter Study Group," *Ann. Thorac. Surg.* Vol. 54, 517–522, 1992.

[2] D. M. Cosgrove III, J. H. Petre, J. L. Waller, J. V. Roth, C. Shepherd, *et al*, "Automated control of postoperative hypertension: a prospective, randomized multicenter study," *Ann. Thorac. Surg.* Vol. 47, 678–682, 1989.

[3] S. A. Hoeksel, J. A. Blom, J. R. Jansen, J. G. Maessen, J. J. Schreuder, "Automated infusion of vasoactive and inotropic drugs to control arterial and pulmonary pressures during cardiac surgery," *Crit. Care Med.* Vol. 27, 2792–2798, 1999.

[4] G. I. Voss, P. G. Katona, H. J. Chizeck, "Adaptive multivariable drug delivery: control of arterial pressure and cardiac output in anesthetized dogs," *IEEE Trans. Biomed. Eng.* Vol. 34, 617–623, 1987.

[5] C. Yu, R. J. Roy, H. Kaufman, B. W. Bequette, "Multiple-model adaptive predictive control of mean arterial pressure and cardiac output," *IEEE Trans. Biomed. Eng.* Vol. 39, 765–778, 1992.

[6] K. Uemura, M. Sugimachi, T. Kawada, A. Kamiya, Y. Jin, *et al.*, "A novel framework of circulatory equilibrium," *Am. J. Physiol. Heart Circ. Physiol.* vol. 286, no. 6, pp. H2376–H2385, Jun. 2004.

[7] K. Uemura, T. Kawada, A. Kamiya, T. Aiba, I. Hidaka, *et al.*, "Prediction of circulatory equilibrium in response to changes in stressed blood volume," *Am. J. Physiol. Heart Circ. Physiol.* vol. 289, no. 1, H301–H307, Jul. 2005.

[8] K. Uemura, A. Kamiya, I. Hidaka, T. Kawada, S. Shimizu, *et al.*, "Automated drug delivery system to control systemic arterial pressure, cardiac output, and left heart filling pressure in acute decompensated heart failure," *J. Appl. Physiol.* vol. 100, no. 4, 1278–1286, Apr. 2006.

[9] K. L. Chien, J. A. Hrones, J. B. Reswick, "On the automatic control of generalized passive systems," *Trans. ASME.* Vol. 74, 175–185, 1952.